
pH-Sensitive Nitroxide Radicals for Studying Inorganic and Organo-Inorganic Materials and Systems

Elena Kovaleva and Leonid Molochnikov

Additional information is available at the end of the chapter

<http://dx.doi.org/10.5772/39119>

1. Introduction

Many inorganic materials are widely used as adsorbents and catalysts. For example, silica gels efficiently absorb vapors and gases in chemical reactors and are applied as filters for the purification of mineral oils and water (Buyanov, 1998). Different aluminum oxide modifications show good adsorption and catalytic properties in many organic reactions due to the presence of active sites on their surface (Lisichkin et al., 2003). TiO₂ gels are widely used in heterogeneous catalysis owing to their enhanced chemical stability, the accessibility of active sites on their surface throughout the reaction volume, simplicity of reaction product separation, and the feasibility of repeated regeneration (Petrov et al., 1998).

The efficiency of these materials mainly depends on the degree of surface development, texture and structural characteristics, availability of active centers, and possibly medium acidity near these centers. The specific surface diminishes on drying in any procedure for the preparation of xerogels. It can be maintained constant by a number of methods, including the use of additions (Ur'ev & Potanin, 1992), for example, powder cellulose (PC) (Shishmakov et al., 2007). Cellulose is a linear high molecular polysaccharide, which forms rigid chain structures due to the inter-molecular hydrogen bonding. It functions in nature as an agent that imparts high mechanical stability to plant tissues (Nikitin, 1962). The deposition of SiO₂ and TiO₂ xerogels on the PC surface affords composite materials (CMs) with a high dispersity of particles (Shishmakov et al., 2010).

The use of hybrid organo-inorganic materials as supports is a new area in the development of new metal-containing catalytic materials. It allows to obtain supports with specific surfaces that are capable of retaining the metallic component of a catalytic system more strongly.

Chitosan, poly-D- β -glucosamine, is a commercially available amino polymer that is a perfect complexing agent, due to the strong donor properties of both the amino and hydroxyl groups (Varma et al., 2004). Chitosan is thus widely used in obtaining various catalytic materials, including those containing Au^0 that are used in the hydroamination of alkenes (Corma et al., 2007); Pd^0 used for the reduction of ketones (Yin et al., 1999); the Pd^0 - Ni^0 bimetallic system, used for carbonylation (Zhang & Xia, 2003); Os (VIII), used for hydroxylation (Huang et al., 2003); Co^{2+} , used for hydration (Xue et al., 2004); and Cu^{2+} , used for the oxidation of catecholamines (Paradossi et al., 1998).

SiO_2 is usually used as the inorganic component for these systems. The obtained hybrid materials are used to create sorbents of 3d-metal ions (Liu et al., 2002); to immobilize enzymes (Airoldi & Monteiro, 2000); as a solid phase for the liquid chromatography of organic compounds (Budanova et al., 2001), including enantiomers (Senso et al., 1999); and to improve the mechanical properties of other polymers (Yeh et al., 2007). Other oxides in combination with chitosan allow us to obtain biosensors based on ZnO substrate (Khan et al., 2008), selective sorbents of fluoride ions based on Al_2O_3 substrate (Viswanathana & Meenakshib, 2010) and magnetic materials based on Fe_3O_4 substrate (Li et al., 2008). Using an organic polymer (e.g., cellulose) as a substrate also has advantages in the sorption of metal ions (Corma et al., 2007). Metal-containing hybrid organo-inorganic materials can also be used as antibacterial composites (Mei et al., 2009), as sorbents of proteins (Shi et al., 2003), and as pervaporation membranes (Varghese et al., 2010).

Nanostructured metal oxides, which are distinguished by extremely developed surface and porosity of particles, are new promising materials for different fields of science and technology, especially, for heterogeneous catalysis and chemistry of adsorption phenomena (Zakharova et al., 2005).

Many sorption and catalytic processes are pH-dependent. Therefore, the determination of acidity and other acid-base characteristics in pores of inorganic, organo-inorganic materials is of great practical interest, since the catalytic and adsorption properties of solid-phase objects are affected by not only the chemical nature of solutions, but also specific conditions inside pores and on the surface of these materials. The mobility of liquid molecules in pores of inorganic sorbents was investigated by some authors using the spin probe method (Borbat et al., 1990; Martini et al., 1985). Recently, a new method was developed for the determination of medium acidity in pores of solids (pH_{int}) by means of pH-sensitive nitroxide radicals (NRs) as spin probes (Molochnikov et al., 1996; Zamaraev et al., 1995). In recent years, this method was used to measure pH_{int} in micropores of various cross-linked organic polyelectrolytes (ion-exchange resins and films) (Molochnikov et al., 1996, 2004) and in pores of some zeolites and kaolin (Zamaraev et al., 1995). We found that pH_{int} inside sorbents differ from the pH of external solutions by 0.8–2.1 units (Molochnikov et al., 1996). The method developed allowed us to study the processes of sorption and hydrolysis in ion-exchange resins and the catalytic properties of Cu^{2+} -containing carboxyl cation exchangers (Kovaleva et al., 2000), to determine ionization constants of functional groups and to give a critical estimation to the regularities previously found for the behavior of adsorbents in aqueous media.

pH-sensitive nitroxide radicals (NR) as labels were also used to determine surface electrical potential (SEP) of different biological objects like phospholipids (SLP) - derivatives of 1,2-dipalmitoyl-sn-glycero-3-phosphothioethanol (PTE) (Voinov et al., 2009) and the mixed bilayers composed of dimyristoylphosphatidylglycerol and dimyristoylphosphatidilcholine (Khramtsov & Weiner, 1988).

This work is aimed to review the applications of pH-sensitive NR as probes and labels for determination of local acidic and electrochemical characteristics of inorganic and organo-inorganic materials and systems such as :

- Al_2O_3 (non-modified and modified with F^- and SO_4^{2-} ions) and TiO_2 as hydrogels and nanopowders doped with Cu(II) (Molochnikov et al., 2007) ;
- pure and Cu^{2+} -containing solid-phase composites based on nanostructured SiO_2 and TiO_2 and powder cellulose (Shishmakov et al., 2010; Parshina et al., 2011) ;
- pure and Co^{2+} -containing hybrid organo-inorganic materials based on the chitosan- SiO_2 , chitosan- Al_2O_3 , and -chitosan-cellulose systems (Mekhaev et al., 2011a, 2011b).

2. Experimental

2.1. Objects of study

$\alpha\text{-Al}_2\text{O}_3$ (basic aluminum oxide), $\gamma\text{-Al}_2\text{O}_3$ and its acid-modified (HF and H_2SO_4) derivatives were supplied by A. M. Volodin. The **IK-02-200 type $\gamma\text{-Al}_2\text{O}_3$** was synthesized by the calcination of aluminum hydroxide at 600°C . $\gamma\text{-Al}_2\text{O}_3$ was modified through the sample impregnation with acids followed by calcination at 600°C that resulted in changes in the acidic properties of its surface (the phase composition and specific surface area of the samples remained unchanged). $\alpha\text{-Al}_2\text{O}_3$ was prepared by the long-term heating of $\gamma\text{-Al}_2\text{O}_3$ to 1300°C . $\gamma\text{-Al}_2\text{O}_3$ and $\alpha\text{-Al}_2\text{O}_3$ had specific surface areas of 220 and 145 m^2/g , and an average pore diameter of 6 nm, respectively. The structural characteristics of the matrices were determined from the isotherms of nitrogen adsorption at 77 K measured on a Micromeritics ASAP 1400 volumetric setup and by mercury porosimetry with a Micromeritics Pore Size 9300 setup in the Institute of Catalysis, Siberian Division, Russian Academy of Sciences.

The technique of synthesis of **TiO_2 hydrogel** through the hydrolysis of a tetrabutyl titanate solution in methanol with water at room temperature and under intensive agitation is given in (Shishmakov et al., 2003). The precipitate was washed out with water until no butanol in washing water was observed and heated to 100°C . The resulting product was **TiO_2 xerogel**.

SiO_2 hydrogel was synthesised by dissolving 10 ml of Na_2SiO_3 (TU 6-15-433-92) in 30 ml of H_2O . Then the hydrolysis of Na_2SiO_3 solution in 30 ml of 10% HCl solution was pursued under intensive agitation. During the reaction of condensation a gelatinous SiO_2 gel and NaCl are formed. The precipitate was filtered off until no chlorine ions in washing water was observed, and dried at 100°C during 24h until it attained a constant weight. The resulting product was **SiO_2 xerogel**.

Powder cellulose (PC) was obtained by hydrolysis of cellulose sulfate (Baikal Cellulose plant, TU OP 13-02794 88-08-91) in 2.5 N hydrochloric acid at 100°C. The hydrolysis was carried out for 2 h. The resulting product was washed on a filter with distilled water to the neutral pH of the washing water and dried at 100°C.

Composite materials (CMs) based on nanostructured TiO₂ and PC called as TiO₂-PC xerogels of 70, 53 and 43 % wt. TiO₂ were prepared by diluting 3 g of tetrabutoxytitanium and 0.5 ; 1 and 1.5 g of PC, respectively, in 3 mL of methanol. The hydrolysis was pursued in 10 mL of water at 20°C under intensive agitation, resulting in the condensation of TiO₂ (PC didn't participate in condensation). The TiO₂ particles formed were deposited on a surface of PC.

Composite materials (CMs) based on nanostructured SiO₂ and PC called as SiO₂-PC xerogels of 68, 52 and 35% wt. were prepared from the solutions of 10 ; 5 ; 5 ml of Na₂SiO₃ and 30 ; 15 ; 15 ml of H₂O which were modified by introducing 2 ; 2 ; 4 g of PC, respectively. The hydrolysis of the first solution were performed in 30 mL of 10 %HCL, and that of other ones was done in 15 mL of 10% HCL.

The precipitates of the CMs prepared were washed out with hot water, filtered and dried at 100 °C during 24h until they attained a constant weight.

The specific surface (S_{sp}) of the synthesized samples was measured using a SORBIMS instrument (ZAO Meta, Novosibirsk) and calculated by the BET procedure. The data are given in Table 1 (Parshina et al., 2011).

	TiO ₂				SiO ₂		
PC, %	0	30	47	57	0	32	65
$S_{sp}, m^2/g$	66	177	226.4	261.9	29.5	145	239

Table 1. The specific surface of the pure xerogels of TiO₂ and SiO₂ and the composites with different percentage of PC

Since the specific surface of powder cellulose did not exceed 1 m²/g, the growth of S_{sp} was caused by the fragmentation of TiO₂ and SiO₂ particles deposited on the PC surface during the synthesis of CMs. According to the absolute values of S_{sp} , the procedure used for the preparation of CMs afforded dioxides with a high degree of dispersity.

Powdered samples **nanostructured TiO₂** were prepared through heating a sol for 1 h at 200°C followed by washing with distilled water to remove residual acid used for the sol stabilization and drying at room temperature. The specific surface area of the samples was 240 m²/g, and the average particle diameter ranged from 4 to 5 nm (Poznyak et al., 1999).

Microcrystalline cellulose (MCC) with an ash content of 0.16% and a humidity of 1.1% produced by JSC Polyex; Basic aluminum oxide; BS-50 silica and chitosan produced by JSC Sonat (Moscow) were used to obtain chitosan-containing ahybride organo-inorganic systems. The degree of deacetylation of chitosan (DD) determined by 1H NMR spectroscopy, its molecular weight as determined by viscosimetry and the ash content were found to be 0.84, 250 kDa and 0.19%, respectively (Mechaev et al., 2011a). The BS-50 type silica had a specific surface area of 45 m²/g and an average diameter of pores of 15 nm (Mekhaev et al., 2011a).

The hybrid chitosan–(SiO₂, Al₂O₃, cellulose) systems were obtained by depositing chitosan on the support surface.

0.3 g (1.8 mmol) of chitosan was dissolved in 14.5 ml of water containing 0.22 ml (3.84 mmol) of acetic acid with constant stirring. The substrate in quantities of 3 g was then added, and the solution was stirred for 30 min more.

1 M NaOH solution was added to the suspension under stirring until the pH value reached 13. The precipitate was filtered, washed until the pH value was 7, and dried at 60°C until it attained a constant weight.

CHN analysis was performed using an automatic analyzer PerkinElmer, Inc. The data are given in Table 1. IR spectra of diffuse reflection were recorded using the PerkinElmer Spectrum One spectrometer.

System	C	H	N	Cl	Co	Formula
MCC-Chitosan	43.08 (43.11)	6.42 (6.35)	0.37 (0.39)	-	-	10C ₆ H ₁₀ O ₅ · 0.5C ₆ H ₁₁ NO ₄ · 3H ₂ O
Al ₂ O ₃ -Chitosan	4.07 (4.01)	1.04 (0.61)	0.46 (0.78)	-	-	16Al ₂ O ₃ · C ₆ H ₁₁ NO ₄
SiO ₂ -Chitosan	4.50 (4.49)	0.94 (0.68)	0.51 (0.87)	-	-	24SiO ₂ · C ₆ H ₁₁ NO ₄
MCC-Chitosan- Co ²⁺ (I)	43.12 (43.12)	6.15 (6.04)	0.59 (0.40)	1.30 (1.28)	1.38 (1.33)	10C ₆ H ₁₀ O ₅ · 0.5C ₆ H ₁₁ NO ₄ · Co _{0.4} (OH) _{0.17} Cl _{0.65}
Al ₂ O ₃ -Chitosan- Co ²⁺ (II)	3.64 (3.82)	0.79 (0.58)	0.47 (0.74)	2.69 (2.63)	2.18 (2.19)	16Al ₂ O ₃ · C ₆ H ₁₁ NO ₄ · 0.7CoCl ₂
SiO ₂ -Chitosan- Co ²⁺ (III)	4.02 (4.26)	0.89 (0.65)	0.58 (0.82)	2.03 (2.02)	3.07 (3.07)	16SiO ₂ · C ₆ H ₁₁ NO ₄ · Co _{0.88} Cl _{0.96}

Table 2. Composition (%) of hybrid systems (calculated values are shown in brackets)

The surface area of the samples was determined by nitrogen adsorption in accordance with the BET method using a TriStar 3000 V.6.03A instrument. The instrumental error was 0.1 m²/g. The size of particles was estimated under the assumption that the particles were spherical.

The surface area (*S_{sp}*) and the diameter of particles (*D*) were found to be 28.9 m²/g and 47 nm; 123.9 m²/g and 7 nm; 2.4 m²/g and 818 nm for chitosan-SiO₂, chitosan-Al₂O₃ and chitosan-MCC hybride systems, respectively.

2.2. Saturation of samples with Cu²⁺ and Co²⁺ ions

2.2.1. Saturation of samples with Cu²⁺ Ions

A 0.1 M NaNO₃ solution (10 ml) was added into weighed samples (200 mg) of nanostructured TiO₂, and the samples were kept for one week at a constant solution pH (5.5) held by adding dilute NaOH and HNO₃ solutions. The sorption of Cu²⁺ ions on nanostructured TiO₂ was performed by exposing samples in Cu(NO₃)₂ solutions (10 ml)

with concentrations of 10^{-4} , 10^{-3} , and 10^{-2} mol/L and ionic strength (μ) of 0.1, which was adjusted using NaNO_3 . Solution pH equal to 4.3 was maintained by the titration with small volumes of NaOH and HNO_3 solutions. After the equilibrium was established, the residual amount of Cu^{2+} ions the equilibrium solutions was measured to determine the amount of sorbed Cu^{2+} . Then, TiO_2 was separated from the solutions by centrifugation. The samples were washed twice with a 0.1 M NaNO_3 solution (pH 4.3) to remove adsorbed Cu^{2+} -ions.

Cu^{2+} ions were sorbed on TiO_2 hydrogel from CuCl_2 and $\text{Cu}(\text{NO}_3)_2$ with subsequent its removal by filtration and drying at 20°C for 3 days upto constant weights of the precipitates. A volume of solution and a mass of hydrogel were changed to vary the content of Cu^{2+} ions in the phase of the studied TiO_2 hydrogel, which was determined by the atomic absorption method on a Perkin Elmer 403 spectrometer. As the ESR spectra of Cu^{2+} -containing hydrated gels are difficult to record, hydrogel samples filtered and dried at room temperature were used. Preliminary experiments were performed to select the sample drying conditions preventing the structural changes of the complexes formed.

Cu^{2+} - containing composites based nanostructured SiO_2 , TiO_2 , and cellulose powder were prepared by sorption of Cu^{2+} ions on a hydrogel from an aqueous solution of $\text{CuCl}_2 \cdot 2\text{H}_2\text{O}$. The volumes of hydrogels of the samples studied were calculated from the masses of xerogels obtained by hydrogels drying. For preparation of Cu^{2+} -containing TiO_2 and SiO_2 xerogels and the related CMs, a 0.01 g $\text{CuCl}_2 \cdot 2\text{H}_2\text{O}$ containing 0.059 mmol of Cu^{2+} ions and 2 ml of H_2O and the calculated volumes of hydrogels prepared were added into flasks. The samples were kept in the contact with a Cu^{2+} -containing solution about 24 h upto the equilibrium was established. Then, the residual amounts of Cu^{2+} ions in the equilibrium solutions was measured to determine the amount of sorbed Cu^{2+} ions. The initial and residual amounts of Cu^{2+} -ions in a solution were measured using colorimeter KFK-2MP.

2.2.2. *Synthesis and characterization of the Cobalt-Containing Chitosan hybrid systems*

Cobalt-Containing Chitosan-Supported Systems were synthesised through stirring a mixture containing 0.24 g of $\text{CoCl}_2 \cdot 6\text{H}_2\text{O}$, 2 g of chitosan-supported hybrid system and 20 ml of ethanol under reflux condenser for 24 h. The obtained cake was filtered off, rinsed with ethanol (15 ml \times 3 times) and dried at room temperature until the weight became constant. The elemental compositions of the hybrid system surfaces were determined using an analytical setup based on a VEGA II LMH scanning electron microscope and an INCA ENERGY energy dispersive microanalysis system (Mekhaev et al., 2011a, 2011b). The data are shown in Table 2.

2.3. pH probes

The pH values of solutions inside pores and near the surface of the studied inorganic and organo-inorganic materials were determined using spin probes, namely, pH-sensitive NRs of the imidazoline (R1, R2) and imidazolidine (R3) types (Table 3), which were synthesized at the Novosibirsk Institute of Organic Chemistry, Siberian Branch, Russian Academy of Sciences (Volodarskii et al., 1988; Khramtsov et al., 1998; Kirilyuk et al., 2005).

2.4. Recording and processing of the ESR spectra of NR

The ESR spectra were recorded on a PS 100.X ESR spectrometer (ADANI, Belarus) in a three-centimeter (X) wavelength range at room temperature. Quartz sample holders with an internal diameter of 3.5 mm were used for solid samples. Solution spectra were recorded using quartz capillaries.

Figure 1 shows characteristic ESR spectra of the pH-sensitive NR in aqueous solutions. According to the ESR theory, isotropic signals are induced by the fast-motivated NR molecules (correlation times of 10^{-10} s and less) and present the triplet of fine lines. Depending on solution pH, NR can be in protonated (RH^+), deprotonated (R), or intermediate (mixed) forms. Because hyperfine splitting constants a_N for RH^+ and R forms of the radicals are different (Table 3), in their ESR spectra, the distance a between the low and central-field component of the triplet increases gradually with pH of a solution, from the values characteristic of the RH^+ form to those typical of the R form (Fig. 1). This characteristic is a superposition of hyperfine splitting constants (a_N) characterizing protonated and deprotonated forms of the nitroxide radical. From the results of measuring a values during titration, the calibration curves reflecting the dependences a vs. pH were plotted for each NR used (for example, see Fig. 2, 3 curve 1). In order to plot the calibration curves, NR solutions (10^{-4} mol/l; $\mu = 0.1$) were titrated either with dilute HCl and KOH solutions (used for all the samples, excepting hybride systems) (Molochnikov et al., 2007; Parshina et al., 2011; Shishmakov et al., 2010) or citrate-phosphate (pH 3.5-7.8) and citrate-salt (pH 1.6-4.8) buffer solutions (used for hybride systems) (Mekhaev et al., 2011a, 2011b). to vary the pH within the range of NR sensitivity of 2.5 – 7.5.

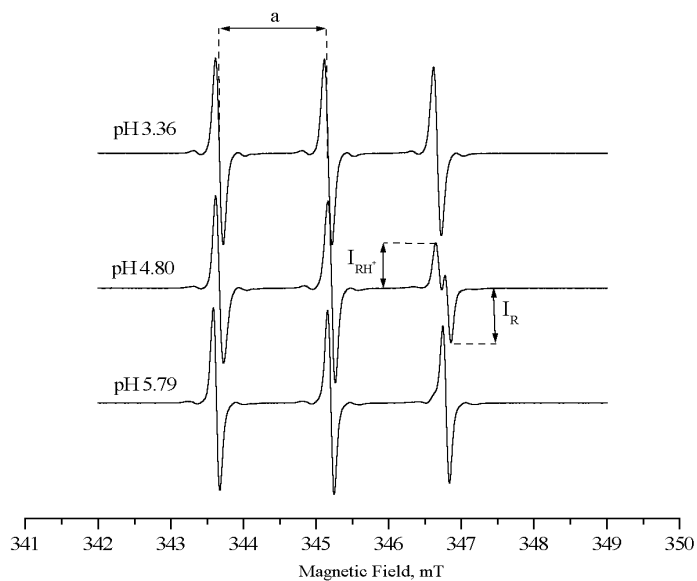


Figure 1. The ESR spectra of the aqueous solution of NR R3 at different pH in the X range of wavelengths at 293K. I_{RH^+} and I_{R} are the intensities of ESR peaks for RH^+ and R forms of the radical, respectively

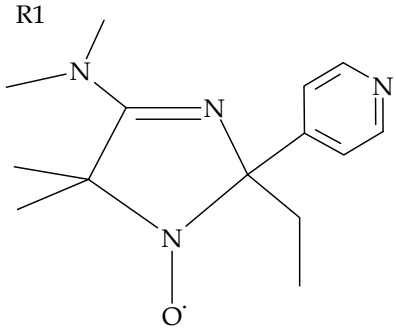
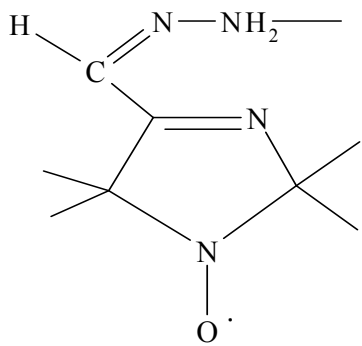
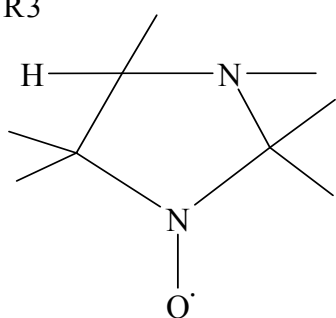
Radical	pK _a (± 0.1)	g-factor (± 0.0001)		a _N (± 0.006 mT)	
		R	RH ⁺	R	RH ⁺
<p>R1</p> 	3.15 4.89	2.0048	2.0051	1.520	1.390
<p>R2</p> 	3.55	2.0048	2.0051	1.590	1.515
<p>R3</p> 	4.70	2.0048	2.0051	1.590	1.485

Table 3. ESR parameters and pK_a values of nitroxide radicals used

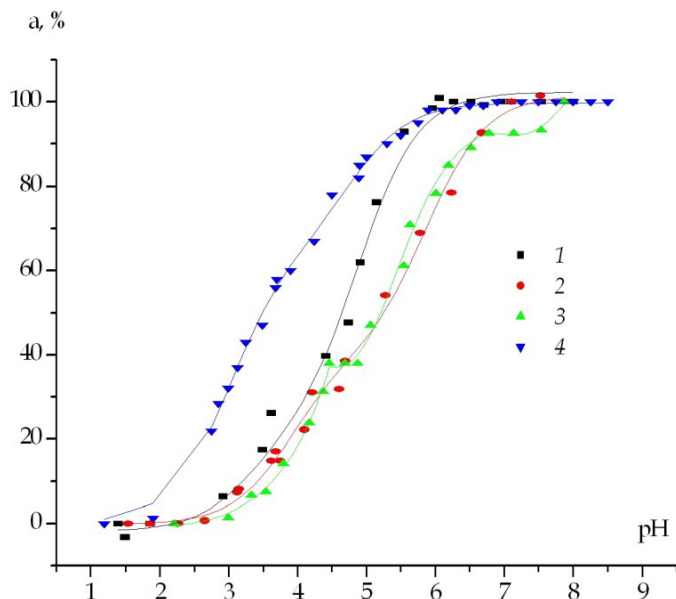


Figure 2. Titration curves for NR R1 in bulk aqueous solution (calibration curve) (1), α - Al_2O_3 (2), the BS-50 SiO_2 (3) and γ - Al_2O_3 (4). $a, \% = ((a - a_{\text{NRH}^+}) / (a_{\text{NR}} - a_{\text{NRH}^+})) \times 100\%$

2.5. Determination of pH in the pore and near the sample surface using pH-sensitive spin probes

An aqueous KCl solution (10 ml) with an ionic strength of 0.1 was added to an oxide sample (200 mg) and the mixture was allowed to stand for a preset time. Then, the solution was thoroughly decanted and an NR solution (10^{-4} mol/L, $\mu = 0.1$) was added to the sample. In some cases, required initial pH values of radical solution were obtained by preliminary mixing of HCl and KOH solutions. After the equilibrium was established, the suspension was titrated with HCl and KOH (HNO_3 and NaOH) solutions to plot the titration curve for the NR present in the sample.

For chitosan cobalt-containing hybrid systems and solid-phase composites based on SiO_2 , TiO_2 and cellulose powder the method of multiply batches was used: 0.05 g of sample was kept in 5 ml of buffer aqueous solution containing nitroxide radicals for 2 days (established experimentally). The solution was then decanted.

The pH values of the equilibrium solutions (pH_{ext}) over the samples were measured using a Mettler Toledo pH meter (Switzerland) with an accuracy of 0.01 units. The samples separated from the solutions by centrifugation or filtration were placed into unsealed quartz ampules and their ESR spectra were recorded. After measuring the a distances in the ESR spectra of corresponding radicals located in the samples (Fig. 4), the pH_{int} values of the studied materials were determined using the calibration curves (Fig. 2,3).

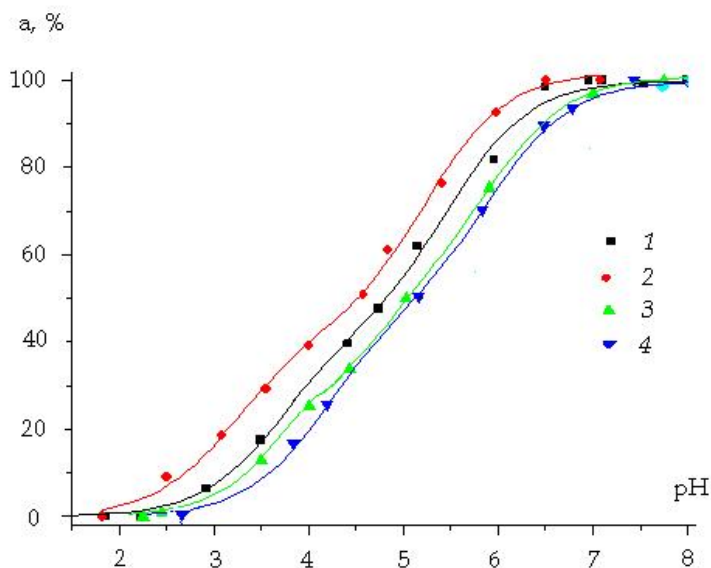
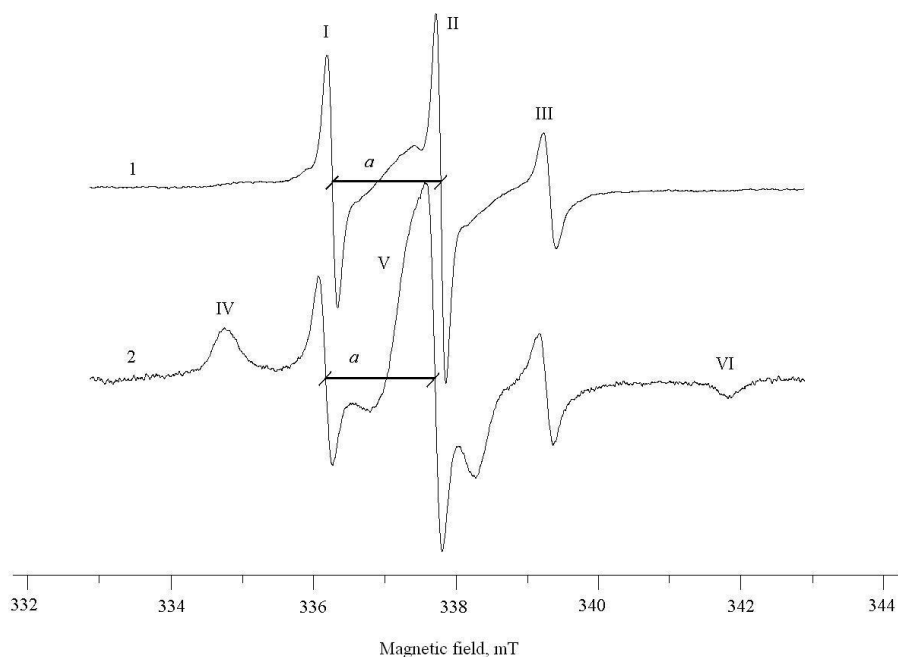


Figure 3. Titration curves for NR R1 in bulk aqueous solution (calibration curve) (1), PC (2), SiO_2 (3) and TiO_2 (4) xerogels. $a, \% = ((a - a_{\text{NRH}^+}) / (a_{\text{NR}} - a_{\text{NRH}^+})) \times 100\%$

As can be seen from Fig. 4, the ESR spectra of NR in the samples studied represent the superpositions of three components of an isotropic signal of the probes in aqueous solutions inside pores and a spectrum of the probes immobilized on the surface of the objects studied. For determination of pH_{int} values, only the isotropic signals in the ESR spectra were used.



I, II, II – components of an isotropic spectrum ; IV, V, VI – components of the spectrum of the immobilized probes

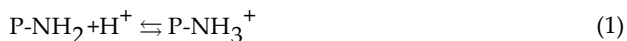
Figure 4. The ESR spectra of NR R1 in the samples of CMs SiO₂-PC (68% wt.SiO₂) at pH 7.8 (1) and pH 3.7(2)

3. Results and discussion. Acid-base equilibria of inorganic and organo-inorganic materials and systems

3.1. Inorganic oxide materials

3.1.1. Pure oxides

The comparison of the titration curves for NR R1 radical in γ -Al₂O₃, α -Al₂O₃, the BS-50 type SiO₂ and TiO₂ and SiO₂ xerogels with the calibration curve of this NR (Fig. 2, 3) indicates that for γ -Al₂O₃, the curve is shifted to the left, and for other samples, to the right. As was shown previously for organic sorbents (Molochnikov et al., 2004), the left- side shift of the titration curves for the NRs used is characteristic of anionites in acidic solutions in the pH range, where amino groups bind hydrogen ions, for example,

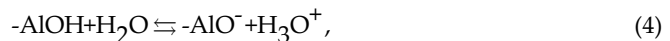
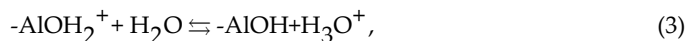


where P is the sorbent matrix. At the same time, the shift in the titration curves to the right is related to the dissociation of acidic functional groups of cationites, for example, a carboxylic one,



Thus, the shift of the titration curve of R1 to the left observed for $\gamma\text{-Al}_2\text{O}_3$ indicates the binding of H^+ ions with the surface (pH_{intr} is higher than solution pH) and to a positive charge of $\gamma\text{-Al}_2\text{O}_3$ surface, while the right-hand side shift of the titration curve of this NR in SiO_2 gel suggests the release of H^+ ions and, consequently, a negative surface charge.

According to the data reported in (Hubbard, 2002) the acidic dissociation of hydrated aluminum oxide occurs in two stages, which can be described by the following equations:



The pK_a values of these equilibria ($\text{pK}_{a1} = 5.87$ and $\text{pK}_{a2} = 7.50$) are given in (Lidin et al., 1987). Using NR, we can determine only pH values relevant to the ascending part of its S-shaped calibration curve (Fig. 2, 3 curve 1), i.e., the range, in which variations in a parameter correspond to variations in pH. The range of pH values appropriate to the ascending part of the calibration curve for a given NR is referred to as the zone of its sensitivity. The sensitivity zone of NR R1 falls in the pH range from 2.5 to 6.5 (Fig. 2, 3). If the above data on pK_a reflect (even if qualitatively) the pK_a of functional group dissociation for $\gamma\text{-Al}_2\text{O}_3$ studied, then the comparison of the sensitivity zone of NR R1 with pK_a values indicates that the use of NR allows one to study only the pH range in which $\gamma\text{-Al}_2\text{O}_3$ either has a positive charge or is electrically neutral. On the other hand, there are data on the point of zero charge (PZC) for Al_2O_3 in the literature.

For example, as was shown previously, the PZC of an Al_2O_3 sample kept in water for a long time was equal to 9.2, and for Al_2O_3 treated at 1400°C , the PZC decreased to 6.7 (Robinson et al., 1964). The first value corresponds to $\gamma\text{-Al}_2\text{O}_3$, and the second one, to $\alpha\text{-Al}_2\text{O}_3$. For hydrated Al_2O_3 the PZC was found to be equal to 8, and it decreases as a result of the modification of Al_2O_3 surface with alkyl phosphate-based surfactants (Jeon et al., 1996). Moreover, these data suggest that, in the studied pH range, the surface of $\gamma\text{-Al}_2\text{O}_3$ has a positive charge that is in accordance with the shift of its titration curve to the left.

The pH_{intr} of the sorbents differ from the pH_{ext} by 0.5–1.5 units (Table 3). Smaller pH_{intr} values compared to pH of the external solutions for all the studied samples (except for $\gamma\text{-Al}_2\text{O}_3$) are indicative of the shift in titration curves of NR R1 to the right relative to the calibration curve, similarly to that demonstrated in Fig. 2, 3 all the samples excepting $\gamma\text{-Al}_2\text{O}_3$.

It should be noted that the pH_{intr} value determined in this study for the hydrated $\alpha\text{-Al}_2\text{O}_3$ is in good agreement with the PZC value found in (Robinson et al., 1964). From the data given in Table 3 we notice that in all the studied samples excepting $\gamma\text{-Al}_2\text{O}_3$ acidic centers

predominate. However, the acidity of these centers is rather weak; their pK_a of dissociation are presumably close to 6. Only when strongly acidic sulfate residues appear in Al_2O_3 , a drastic decrease in pH_{int} is observed as a result of their dissociation. It should be noted that the same decrease in pH_{int} of TiO_2 hydrogel results from the sorption of Cu^{2+} ions by the hydrogel, which leads to the ion-exchange displacement of H^+ ions (Fig. 5).

Sample	$pH_{ext} (\pm 0.01)$	$pH_{int} (\pm 0.1)$
$\alpha - Al_2O_3$	7.72	6.6
$Al_2O_3 - F^-$	6.9	6.4
$Al_2O_3 - SO_4^{2-}$	4.9	3.8
$\gamma - Al_2O_3$	7.16	>7.3
TiO_2 -hydrogel	7.0	5.5
BS-50 type SiO_2	7.5	5.7
TiO_2 -xerogel	7.0	6.1
SiO_2 -xerogel	7.0	6.3

Table 4. pH values of the external bulk solution of NR R1 and in the pores and near a surface of the inorganic materials studied

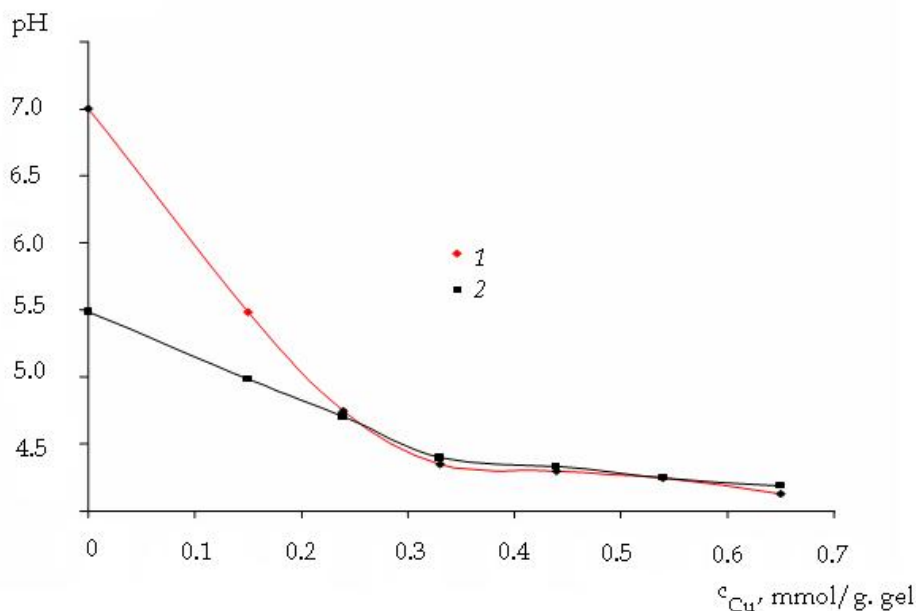


Figure 5. The pH values of a $CuCl_2$ equilibrium solution (pH_{ext}) (1) and a solution inside TiO_2 hydrogel (pH_{int}) (2) vs. the amount of sorbed Cu^{2+} (c_{Cu})

The titration curves of radicals occurring in organic sorbents are characterized by the presence of horizontal plateaus corresponding to constant pH_{int} (parameter a remains unchanged), when the pH of the external solution increases (Molochnikov et al., 2004). The

presence of the horizontal plateaus on the titration curves is related to the consumption of the titrant solution for the neutralization of functional groups of ionites. There was found no horizontal plateau on the titration curve of NR R1 in γ -Al₂O₃ within its zone of sensitivity (Fig.2). This fact can be explained either by the presence of a small number of acidic functional groups in γ -Al₂O₃ or by noncoincidence of pK_a values of these acid groups with the zone of sensitivity of the radical used. Based on our experimental data, it is difficult to make a conclusion in favor of any of these assumptions.

It should be noted that the titration curve of NR R1 in the BS-50 SiO₂ contains two horizontal plateaus corresponding two constant pH_{int} determined near the SiO₂ surface when the pH of the external solution is changed (pH_{ext}) (Fig.2, curve 3). These plateaus are referred to as the titration process of functional groups on the surface (Golovkina et al., 2008). The pK_a values for these groups were determined from the titration curves, and were pK_{a1} = 4.4–4.7 and pK_{a2} = 6.5–6.8. According to (Long et al., 1999 ; Zhao et al., 1997, 1998) amorphous SiO₂ contains groups of three types: silanol, silandiol, and siloxane groups in a ratio of 59.2, 14.7, and 26.1%, respectively. We can therefore assume that the lower and longer horizontal plateau reflects the titration process of silanol functional groups on the SiO₂ surface, and the upper plateau corresponds to silandiol groups. According to (Méndez et al., 2003), the intervals of changes in the dissociation constants are pK₁ = 3.51–4.65 and pK₂ = 6.17–6.84, respectively. The same values of constants of dissociation for silanol and silandiol groups of silica were measured and published in (Nawrocki, 1997 ; Neue, 2000). The presence of silanol and silandiol groups on the surface of the studied SiO₂ was thus identified.

From two types of the xerogels studied (TiO₂ and SiO₂) electrical potential of TiO₂ xerogel is slightly more than that of SiO₂ xerogel (Fig.3). There was found a small horizontal plateau in the range of pH_{intr} between 3.75 and 4.25 on the titration curve for NR R1 near the SiO₂ surface. From this plateau pK_a values for silanol groups were determined. They were found to be equal to 3.95 ± 0,07 within the zone of constant pH_{int} values (Molochnikov et al., 1996). The measured values of pK_a are in good agreement with those determined before for silicas using chromatography (Méndez et al., 2003) and the method of pH probe in different silica-containing samples (Golovkina et al., 2008). At lesser pH values this curve goes near (but slightly righter) than the calibration curve of the above-mentioned NR. As seen from the figure, the surface of SiO₂ xerogel carries a small negative charge which is characteristic for the sample before titrating silanol groups. The lack of horizontal plateaus on the titration curves of NR R1 for the TiO₂ xerogel indicates the fact of titration of its functional groups at pH above 7. It can be explained by the presence of mainly terminal OH⁻ groups with basic properties on a surface of TiO₂ xerogel. The range of their titration lies above the zone of sensitivity of the NR used.

When studying acidity inside organic sorbents or hydrogels, pH probes are placed into water, which penetrates into a solid due to sample swelling. In this case, the probes occur in water environment far away from the chains of organic (synthetic ion-exchange resins) or inorganic (TiO₂ and SiO₂ hydrogel, xerogel) polymers.

The particles of nanostructured oxides in diameter of several nm possess extremely large surface (the ratio of the number of atoms on the surface of a nanoparticle to the number of atoms located inside the particle is equal to 1/7). Therefore, a pH-sensitive NR surrounded by water molecules can approach the hydrated surface of nanoparticles rather closely. It was expected that they as probes and labels would appear to be sensitive to SEP, which would make it possible to estimate its value.

The dependences of NR ionization constants on the surface electric potentials and the polarity of media were reported by Fromherz (Fromherz, 1989) and Khramtsov et al. (Khramtsov et al., 1992) for fluorescent pH indicators and for pH-sensitive NRs, respectively, as follows:

$$\Delta pK_a = \Delta pK_a^{el} + \Delta pK_a^{pol} \quad (5)$$

where ΔpK_a is the total shift in the pKa of an NR occurring in a sample relative to that of the NR in an aqueous solution and ΔpK_a^{el} and ΔpK_a^{pol} are the shifts in the pKa of the NR occurring in the sample, which are due to the electric potential arising on the sample surface and to a change in the polarity of the medium relative to the polarity of the NR aqueous solution, respectively.

$$\Delta pK_a^{el} = -e \times \varphi / 2.3k \times T \quad (6)$$

$$\Delta pK_a^{pol} = b \times (\varepsilon - \varepsilon_{HOH}) \quad (7)$$

where φ is the electrostatic potential, e is the electron charge, k is the Boltzmann constant, T is absolute temperature, b is a proportionality coefficient dependent on the radical nature, ε is the medium permittivity, and ε_{HOH} is the permittivity of water. Figures 6 and 7 demonstrate the results of studying nano-structured TiO₂. The measurements were performed using R3 probe at pH \approx 5.5, which was close to the PZC of TiO₂ (5.7) (Poznyak et al., 1999), and R2 probe at pH \approx 4.3. Near the surface of TiO₂ nanostructured particles, the titration curves of the radicals are shifted to the left, whereas, for TiO₂ hydrogel and xerogel (Fig.3), a shift to the right was observed. At present, we can not find any explanation for such principal different shift in the titration curves for TiO₂-based samples. The TiO₂ hydrogel obtained by hydrolysis was washed out with water, removing acidic components of the initial salts. Hereafter, the samples were prepared at different drying temperatures. The samples of xerogels and nanostructured oxides were dried at 100°C and 200°C, respectively.

As was mentioned above, the shift of the titration curve for γ -Al₂O₃ to the left corresponds to the positive charge of the particle surface that, in principle, correlates with the data obtained at pH below PZC. The left-shift (toward more acidic solutions) of the titration curve of the probe located near the surface of TiO₂ nanoparticles indicates that the surface electric potential is also positive. No changes were found in the hyperfine splitting constants a_N for both deprotonated and protonated R3 radicals (Fig. 6). The curves of titration of NR

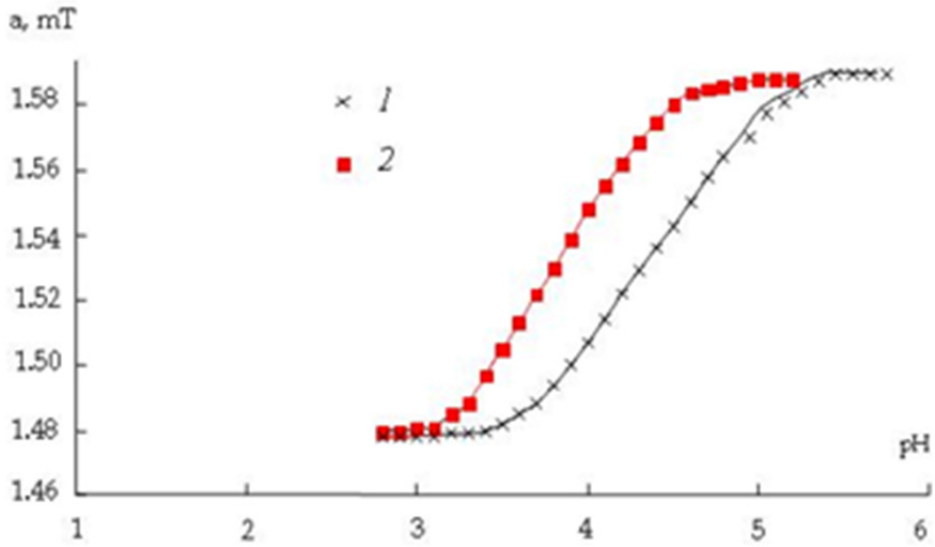


Figure 6. Titration curves for NR R3 in bulk aqueous solution (calibration curve) (1) and near the surface of nanostructured TiO_2 (2) at 25°C and $\mu = 0.1$

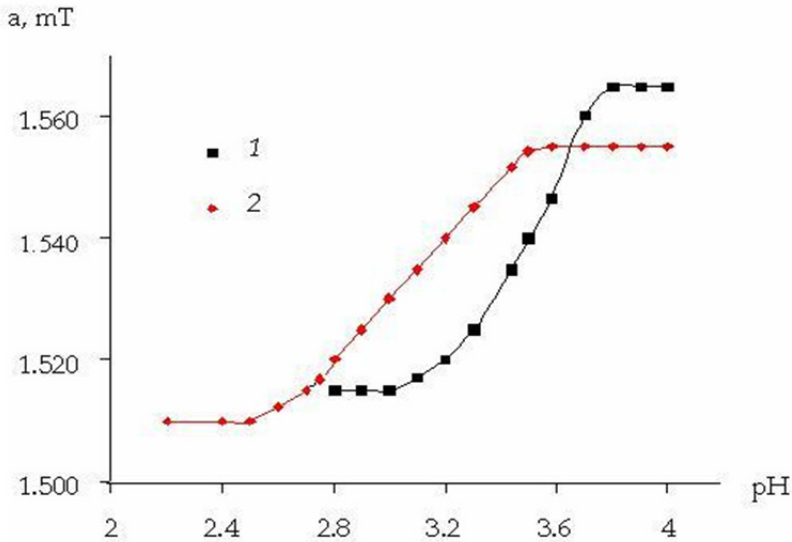


Figure 7. Titration curves for NR R2 (1) in bulk aqueous solution and (2) near the surface of nanostructured TiO_2 at 25°C and $\mu = 0.1$. The amount of Cu^{2+} ions sorbed in the pores of TiO_2 is 0.36 mmol/g of the sample

R3 in the solution (curve 1) and near the surface of the nanostructured TiO₂ (curve 2) begin and end at the same value of parameter a characterizing the hyperfine splitting constant a_N for the protonated and deprotonated forms of NR. This fact shows that there are no changes in the polarity of the medium on the surface of nanostructured TiO₂ relative to the external solution, and the term ΔpK_{a}^{pol} calculated by formula (7) is reduced to zero (Khramtsov et al., 1992). Thus, the shift in pK_a is determined by the electric potential of nanoparticle surface alone ($\Delta pK_a = \Delta pK_a^{el}$). The calculation by formula (6) gives $\varphi = 31.7$ mV at the point of R3 probe location. It should be stressed that the calculated φ value is not the electric potential of TiO₂ nanoparticle surface, but it only characterizes the electric field generated by a nanoparticle at the site where the radical fragment $-N-O\bullet$ of R3 probe is located.

3.1.2. Cu²⁺-containing samples

For TiO₂ hydrogel, pH values of the external solution, which is in contact with the hydrogel (pH_{ext}), and of those inside the hydrogel (pH_{int}) during the sorption of Cu²⁺ ions from copper(II) chloride and nitrate solutions are found to be different (Fig. 5). It was observed that the anions of these copper(II) salts had no effect on the acidity of a medium. In the process of sorption Cu²⁺ ions are involved in the chemical interaction with the active centers of the hydrogel (Kharchuk et al., 2004) that manifests itself both in the parameters of the ESR spectra of Cu²⁺ in the hydrogel and in the impossibility of washing out sorbed Cu²⁺ ions from the hydrogel by Na⁺ and Ca²⁺ nitrate solutions. According to the data obtained, initially, pH_{int} is lower by 1.5 units than pH_{ext} (Table 3). As the amount of Cu²⁺ ions in the hydrogel grows, pH_{int} decreases (Fig. 5), and, beginning with an amount of 0.24 mmol/g of the gel, it coincides with pH_{ext}. Thus, the acidity inside the original hydrogel sample is considerably lower than that of the equilibrium external solution. Similar regularities were found for granulated organic ion-exchange resins (Kovaleva et al., 2000). For KB-2 × 4 cationite in a mixed H⁺-Na⁺ form, it was found that in the process of absorption of copper, the acidity of the external solution diminishes, while the acidity inside the sorbent remains unchanged until a certain amount of Cu²⁺ ions in the ionite is attained, with this content being dependent on the fraction of Na⁺ form of the cationite. When this value is exceeded, the acidity inside the sorbent begins to decrease and pH_{ext} and pH_{int} values for the ionite become equal at a certain degree of saturating with Cu²⁺ ions. For TiO₂ hydrogel, the equalization of pH values is also observed, but the horizontal plateau with a constant pH_{int} value on the titration curve of NR is not observed. The constant pH_{int} values for KB-2 × 4 cationite are explained by the buffer properties of its H⁺-Na⁺ mixed form. TiO₂ hydrogel has no buffer properties, and the acidity increases smoothly with a rise in the amount of sorbed Cu²⁺ ions.

For nanostructural TiO₂, in the presence of sorbed Cu²⁺ ions, at pH close to 4.3 (Fig. 7), like in the case of pure nano-TiO₂ (Fig. 6), a shift of the titration curve toward lower pH values is observed; however, the hyperfine splitting constant a_N decreases (the titration curve is shifted downward). The decrease in a_N is probably related to a lower polarity (the effective permittivity of the medium) near the nanoparticle surface where the probe is located. The theory predicts that the permittivity of a medium must have the same effect on both

electroneutral (the deprotonated form of the radical) and charged (the protonated form) species (Griffith et al., 1974). We found that the rise in the Cu^{2+} amount from 0 to 0.36 mmol/g. of the gel results in an increase in the ΔpK_a value. The shift of this curve (ΔpK_a) to the left is significantly smaller than for NR R3, although the change from the PZC to pH 4.3 and the incorporation of Cu^{2+} ions must enhance the positive charge of the nanoparticle surface and, according to formula (6), increase in ΔpK_a . In accordance with formula (7), a reduction in the permittivity near the surface of TiO_2 particles compared to ϵ_{HOH} , which causes the observed decrease in a_N , must also shift the titration curve to the left.

Hence, the explicit inconsistency between the determined ΔpK_a values for NR R2 and NR R3 radicals and the theoretical predictions is established. We relate this difference to a larger distance of NR R2 from the surface compared to NR R3; this is possible because NR R2 has a substituent in position 4, which is presumably positioned toward the surface due to the tendency of its amino groups to protonation (or complexation with Cu^{2+} ions sorbed on the surface). Thus, the $-\text{N}-\text{O}\bullet$ fragment of the radical turns out to be removed from the surface of TiO_2 by the chain length of this substituent. The electric potential induced on the $-\text{N}-\text{O}\bullet$ fragment will decrease with the distance from the surface and will be inversely proportional to the distance from this surface, when it is represented as, for example, a plane. The small NR R3 radical can approach the nanoparticle surface much closer and, therefore, it is affected more strongly by the electrostatic potential of the TiO_2 surface. The sorption of Cu^{2+} ions on the surface of nanoparticles increases the charge of the latter. The observed shift of the titration curve (Fig. 7) and the broadening of the ESR spectra of these radicals attest to the orientation of the substituent in position 4 of NR R2 toward the surface and to the interaction between amino groups of the substituent and the Cu^{2+} ions sorbed on the nanoparticle surface.

3.2. Organic supports of composite and hybrid materials

For PC and MCC, the titration curves of NR R1 were found to be shifted to the left of the calibration curve (Fig. 2, 3), indicating a positive charge on the surface (Kovaleva et al., 2000; Molochnikov et al., 2007). Hydroxyl groups of cellulose most likely play the role of surface bases whose protonation gives the surface a positive charge.

3.3. Solid-phase composites based on SiO_2 , TiO_2 and cellulose powder

3.3.1. Pure systems

As shown in Fig. 8 and 9, the titration curves of NR R1 in the CMs TiO_2 – PC with 70 (not shown) and 53 % wt. TiO_2 and in the SiO_2 – PC with 68 and 35 % wt. SiO_2 (unprotonated parts) are shifted to the right relative to the calibration curve, as in the case of TiO_2 and SiO_2 xerogels. For CMs based on SiO_2 , TiO_2 and cellulose powder $\Delta\text{pH} = \text{pH}_{\text{ext}} - \text{pH}_{\text{int}}$ decreased (the curves are shifted to the left relative to those of pure xerogels) as the PC content in the samples increased; this corresponds to a decrease in the negative charge of the CM surface. This is because of the lower acidity of cellulose compared to the acidity of the solution (cellulose has basic alcohol functional groups in its structure) and the positive charge of its surface (Parshina, 2011).

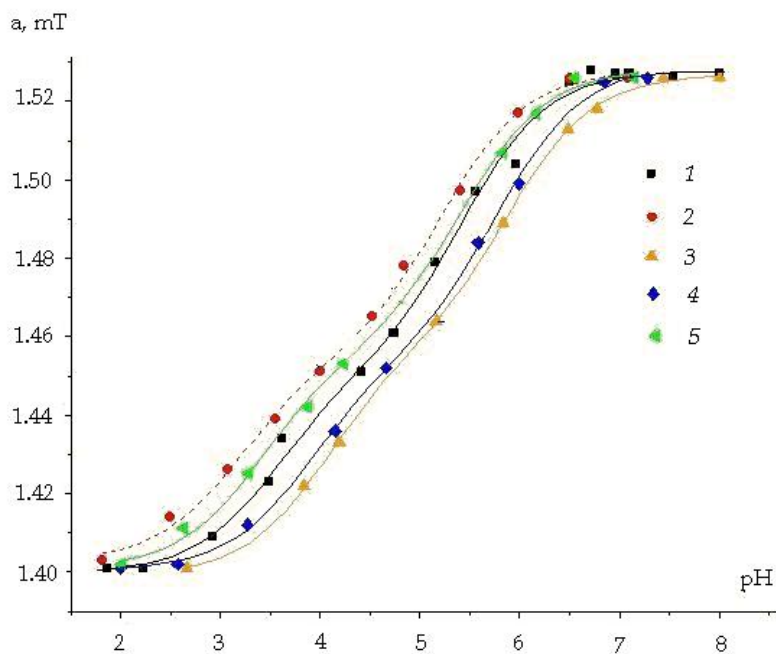


Figure 8. Titration curves for NR R1 in bulk solution (1), PC (2), TiO₂ xerogel (3) и CMs TiO₂: PC (53% wt. TiO₂) (4) and TiO₂: PC (43% wt. TiO₂) (5)

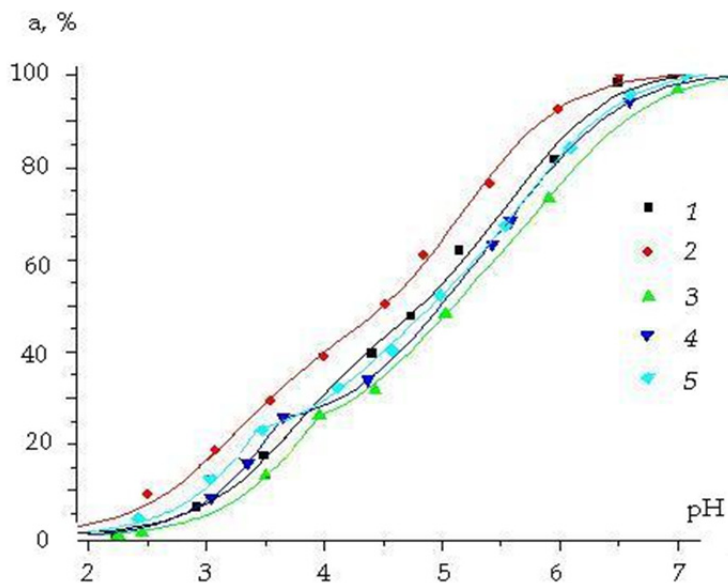


Figure 9. Titration curves for NR R1 in bulk solution (calibration curve) (1), PC (2), SiO₂ xerogel (3) and CMs SiO₂: PC (58% wt. SiO₂) (4) and SiO₂: PC (35% wt. SiO₂) (5). $a, \% = ((a - a_{NRH^+}) / (a_{NR} - a_{NRH^+})) \times 100\%$

This proves that a surface of the composites studied carries lesser negative charge as compared to that of pure xerogels. The left-shift of the curve of NR R1 in CM TiO₂ – PC with 43% wt.TiO₂ relative to the calibration curve can be explained by initial positive charge of the surface of this CM due to binding H⁺ ions. Hence, SEP of CMs based on TiO₂ and PC is varied over a wide range and even changes its sign from negative to positive as an increase in PC content. From the curves plotted, we notice that a decrease in percentage of TiO₂ xerogel in CMs from 53% to 43% leads to a pH_{intr} greater than a pH_{ext}. This fact can be explained by positive charge of a surface of cellulose due to the presence of alcohol groups in its structure.

For all the synthesized CMs based on SiO₂ xerogel and PC after complete protonating silanol groups, the titration curves of NR R1 were shifted to the left relative to the calibration curve and, hence, a surface of the samples studied remained positively charged (Fig.9). Unlike the composites based on TiO₂ and PC, an increase in a percentage of PC in the SiO₂-PC composites leads to changing a surface charge from positive to negative with increasing pH_{ext} (above the horizontal plateau on the titration curves) due to dissociation of functional groups. Thus, the incorporation of PC into the samples doesn't change acidity of silanol groups and doesn't make a polarizing effect on the SiO-H bond. The length of the horizontal plateau slightly increases in the accordance with the amount of silanol groups and the percentage of PC in the CMs based on SiO₂. This can be caused by the increased dispersity of SiO₂ due to rising in S_{sp} of the CMs (Table 1).

By varying the cellulose percentage in the composites and pH_{ext} values, pH_{int} values and SEP can be selected over a wide range. This information is needed for optimization of the conditions for pH-dependent adsorption and catalytic processes through a choice of CM with a certain pH_{int} and SEP as catalyst substrate and adsorbent.

3.3.2. Cu²⁺-containing composites

The sorption of Cu²⁺ on the TiO₂ and SiO₂ xerogels and on the related CMs is accompanied by a change in the pH in their phases. However, the dependences of pH_{ext(int)} vs c_{Cu} (amount of sorbed Cu²⁺ ions) for the above- mentioned types of xerogels and the CMs based have some differences (Fig.10, 11).

From these figures we notice that :

- pH_{int} is different from pH_{ext}, and with no Cu²⁺ in an external solution (c_{Cu} = 0), pH_{ext} is greater than pH_{int}.
- With an increase in the amount of Cu²⁺ in the CMs, both the pH_{ext} and pH_{int} decrease.
- There is a horizontal plateau on the dependences of pH_{int} on c_{Cu} in the range of sorbed Cu²⁺ from 0.15 up to 0.3 mmol Cu²⁺/g. TiO₂, SiO₂ xerogel, within which pH_{int} remains constant with increasing in c_{Cu}.
- At greater c_{Cu} pH_{int} and pH_{ext} come closer and become almost equal.

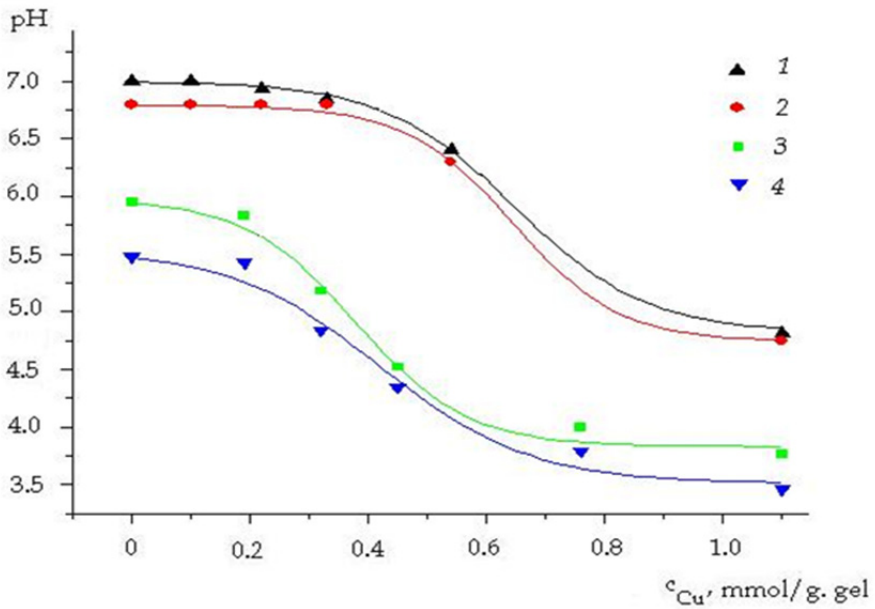


Figure 10. pH of external solution (pH_{ext}) (curves 1,3) and near the surface (pH_{int}) (curves 2,4) of TiO_2 xerogel (curves 1, 2) and the $TiO_2 : PC$ (47% wt. TiO_2) composite (curves 3,4) vs. c_{Cu}

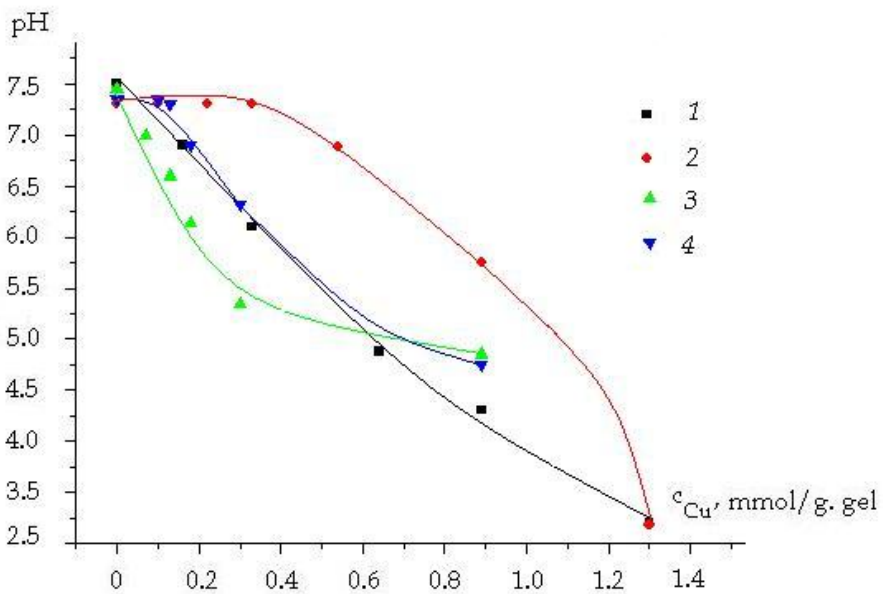


Figure 11. pH of external solution (pH_{ext}) (curves 1,3) and near the surface (pH_{int}) (curves 2,4) of SiO_2 xerogel (curves 1,2) and the $SiO_2 : PC$ (68% wt. SiO_2) composite (curves 3,4) vs. c_{Cu}

The increase in acidity of external solution, first of all, is caused by the hydrolysis of Cu^{2+} at the initial pH_{ext} equal to 6-7 and is accompanied by intense release of H^+ ions. The lesser pH_{int} values as compared to pH_{ext} for both types of xerogels and the related CMs can be explained by a surface negative charge. A surface of the samples studied attracts H^+ ions in its double electrical layer to compensate this charge. Also an increase in acidity of both external and internal (near the surface) solutions is caused by the fact that the sorption of Cu^{2+} ions is accompanied by intense release of H^+ ions into them. The increase in the acidity of a medium due to the competition of H^+ ions almost completely suppresses the ion exchange sorption of Cu^{2+} . An analogous tendency was previously observed for organic ion-exchange resins (as grains) and TiO_2 hydrogel (Kovaleva et al., 2000 ; Molochnikov et al., 2004).

The presence of the horizontal plateaus on the curves pH_{int} vs c_{Cu} (Fig. 9) indicates the buffer properties of the TiO_2 xerogel and the TiO_2 : PC samples by analogy with the same properties of the mixed $\text{H}^+ - \text{Na}^+$ form of the KB-2 \times 4 cationite (Kovaleva et al., 2000). The greater is percentage of PC in a sample, the shorter is the horizontal plateau on the above-mentioned curves. The buffer effect of the TiO_2 xerogel and the related CMs is caused by the existence of some amount of deprotonated functional groups in the samples before the sorption of Cu^{2+} . The complexation of Cu^{2+} ions with these groups occurs first of all and does not lead to the release of H^+ ions, which would reduce both pH_{ext} and pH_{int} . In addition, releasing of hydroxide groups as a result of dissociation of molecules of $\text{Cu}(\text{OH})_2$ responsible for complexation with functional groups of a surface of xerogel can retard decreasing pH with increasing c_{Cu} .

Unlike TiO_2 systems, for SiO_2 and the related CMs pH_{int} values were found to be more than pH_{ext} ones (Fig. 11). Apparently, this difference can be explained by the significant differences in pK_a of functional groups of SiO_2 and TiO_2 oxides. pK_a values of silanol groups (3.95 ± 0.07) are significantly lower than pH_{ext} from which sorption of Cu^{2+} has been conducted. Therefore, silanol groups are completely dissociated and H^+ ions don't exchange with Cu^{2+} ions during complexation. Hence, no functional groups can neutralize OH^- groups forming during breakdown of $\text{Cu}(\text{OH})_2$ molecules. As a result, pH_{int} values (near a surface of samples) have high values.

As the titration curves for TiO_2 -based CMs don't contain the horizontal plateaus as well as pure systems, hence, pK_a values of active acidic centers of a surface of these materials are out of zone of sensitivity of the NR used (greater than 7) (Fig. 8). Therefore, these centers are mainly in the protonated form before sorption of Cu^{2+} -ions. During complexation Cu^{2+} -ions exchange with H^+ ions of functional groups releasing them into external solution. Hence, pH_{int} became less than pH_{ext} . It shows up in a general decrease pH (both pH_{int} and pH_{ext}) with increasing c_{Cu} (Fig. 10).

3.4. Hybrid organo-inorganic materials based on the chitosan– Al_2O_3 , chitosan– SiO_2 , and cellulose –chitosan–systems

Hybrid systems were obtained in accordance with the scheme (Fig.12)

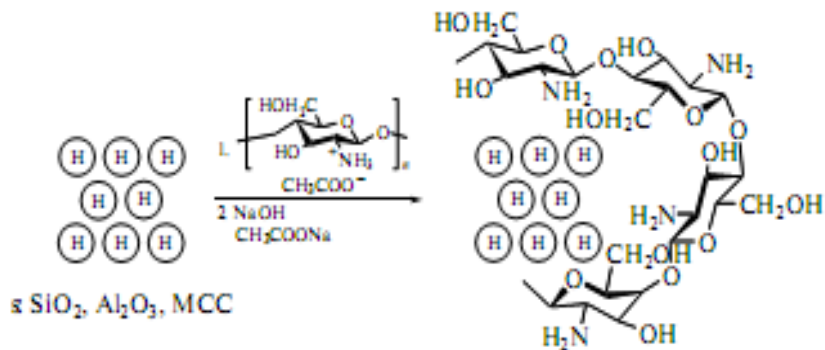


Figure 12. Scheme for obtaining hybrid organo-inorganic materials. s -support

The compositions of the obtained hybrid systems were characterized by elemental analysis (Table 2). According to the obtained data, the reactivity of substrates was different and declined in the order $\text{MCC} > \text{Al}_2\text{O}_3 > \text{SiO}_2$, since the compositions of the obtained hybrids in the case of inorganic oxides do not correspond to the molar ratios of the initial components.

The presence of chitosan molecules on the surface of the obtained systems was confirmed by the IR spectra, which contain characteristic absorption bands at 1652 and 1555 cm^{-1} corresponding to residual acetoamide groups of the polymer.

Since the obtained composites have to be electroneutral, we must assume that in the case of SiO_2 , the substrate, being a weak acid, forms an ionic bond with the chitosan's amino group. In case of Al_2O_3 , the same situation is possible, but some of the chitosan's amino and hydroxyl groups are involved in complex-forming with aluminum. In the case of MCC, the interaction occurs through hydrogen bonds.

NR were used as pH-probes to obtain a more detailed characterization of the surface structure of hybrid systems, their acid-base properties.

A comparison of the ESR spectra of NR R1 in solution and in the samples studied showed that in all cases, there was an isotropic signal which indicated the lack of covalent bonds between the NR and the sample surface and the presence of this radical near the surfaces of particles (Fig. 4, spectrum 1).

3.4.1. Pure hybride systems

Analysis of the structure of the Al_2O_3 -chitosan system according to the adsorbed probe molecules of the nitroxyl radical showed that coating the initial α - Al_2O_3 substrate with chitosan leads to a slight increase in the surface negative charge, as was confirmed by the shift of the NR titration curve to the right (Fig. 13). The titration curves of α - Al_2O_3 and Al_2O_3 -chitosan are not parallel to the calibration curve at low pH values due to the gradual dissolving of α - Al_2O_3 particles in weakly acidic media, as has been noted during investigations of samples containing aluminate ions (Iller, R., 1979 ; Golovkina, 2009).

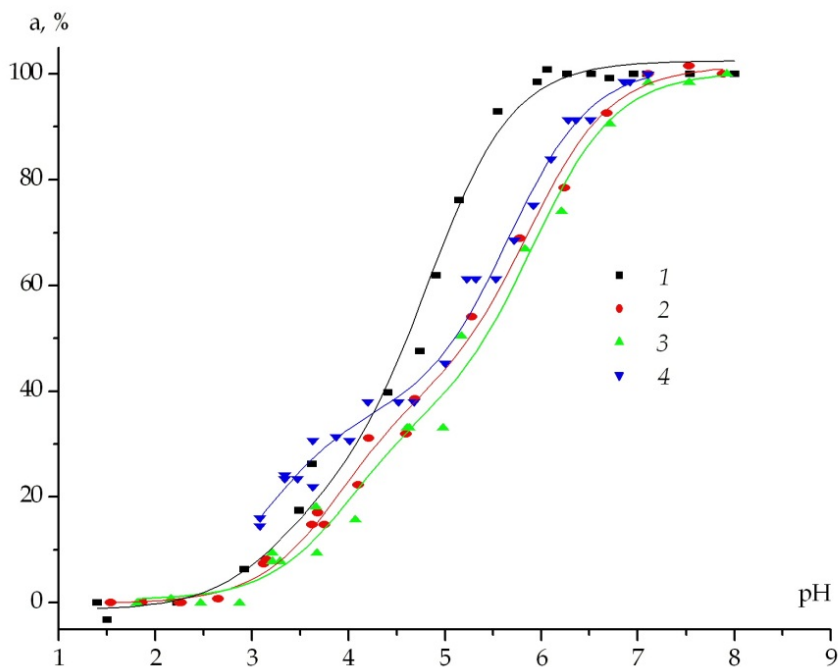


Figure 13. Titration curve for NR R1 in aqueous bulk solution (calibration curve) (1), near the surface of Al_2O_3 (2), hybride Al_2O_3 - chitosan (3) and Al_2O_3 - chitosan- Co^{2+} (4) systems . $a, \% = ((a_{\text{anRH}^+})/(a_{\text{NR}} - a_{\text{anRH}^+})) \times 100\%$

For the SiO_2 -chitosan system, the NR titration curve overlaps the corresponding curve for SiO_2 values within the horizontal section of the titration curve for silandiol groups in the range of high pH (Fig. 14). We can correspondingly claim that in this pH region, the surfaces of the samples all have the same charge, demonstrating that chitosan has no influence on the SiO_2 surface. If pH is decreased below 6, the titration curve for the SiO_2 -chitosan system shifts to the right of the corresponding curve for SiO_2 , indicating the negative charge of the surface. The horizontal plateau of the titration curve for silanol groups is lower in the case of the SiO_2 -chitosan system (pH 4.5–5), and the pK_a value for silanol groups in the presence of chitosan falls slightly. A similar reduction in this parameter has been observed during modification of the surface of mesoporous molecular sieves based on SiO_2 with aluminate and borate ions (Golovkina et al., 2009). Below the titration curve plateau for silanol groups (pH < 4.2), the titration curves of SiO_2 and SiO_2 -chitosan overlap again, indicating a similar surface charge.

The deposition of chitosan on MCC causes the titration curve to shift to the right of to both the calibration curve and the NR titration curve of the initial MCC sample (Fig. 15), demonstrating the negative charge of the surface, as was observed for the Al_2O_3 -chitosan and SiO_2 -chitosan systems. A peculiarity of this substrate is the recharging of the surface, from positive for MCC to negative for the MCC-chitosan system during chitosan

deposition. In this case, the type of change in the surface charge occurring upon a reduction in pH is the same for both the MCC and the MCC–chitosan systems. Changing symbatically with the curve typical of the initial MCC sample, the titration curve for the MCC–chitosan system almost overlaps the calibration curve in the acidic region ($\text{pH} \leq 4.5$). In this pH range, the potential of the MCC–chitosan system surface is therefore close to zero.

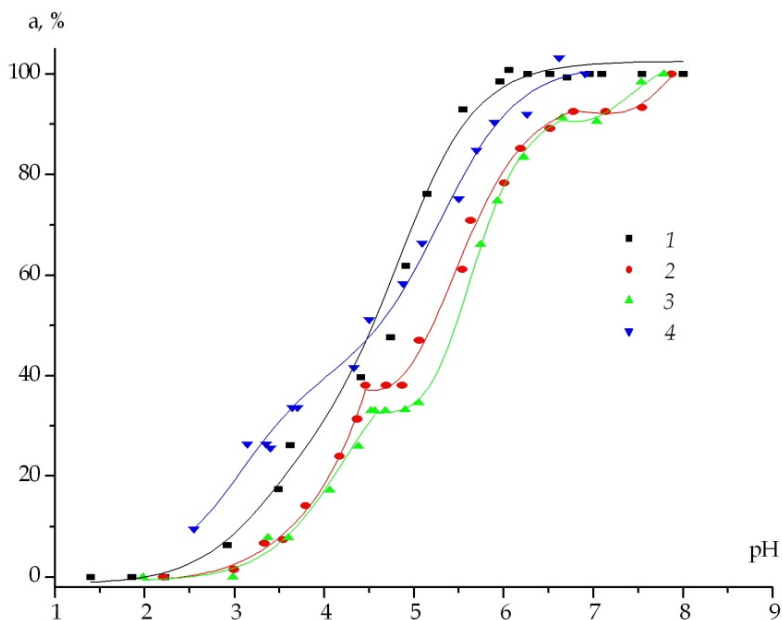


Figure 14. Titration curve for NR R1 in aqueous bulk solution (calibration curve) (1), near the surface of SiO_2 (2), of the hybrid SiO_2 - chitosan (3), of the SiO_2 - chitosan- Co^{2+} (4) systems. $a, \% = ((a_{\text{anRH}^+}) / (a_{\text{NR-anRH}^+})) \times 100\%$

The deposition of chitosan on the substrate always causes the titration curve of the radical near the surface of hybrid material to shift to the right; i.e., it leads to a negative charge on the surface. While the deposition of chitosan leads to relatively slight changes in the surface potential in the case of inorganic substrates, these changes are so great in the case of MCC that they even lead to changes in the surface charge.

Some of differences in the behavior of titration curves for chitosan-containing materials on the inorganic substrates that occur in the range of high pH values could be due to the close pK_a values of the silandiol groups of the SiO_2 substrate ($\text{pK}_a = 6.5\text{--}6.8$) and of the chitosan ($\text{pK}_a = 6.42$ (Skorik et al., 2003)). When the pH falls, amino groups of chitosan or silandiol groups become protonated and form hydrogen bonds with one another. As a result, the charge of the initial substrate surface and that of the hybrid material become similar. During further protonation of silandiol and amino groups at the same pH range, this interaction becomes impossible, and the surface charge of the SiO_2 -chitosan hybrid material becomes more negative than that of the SiO_2 .

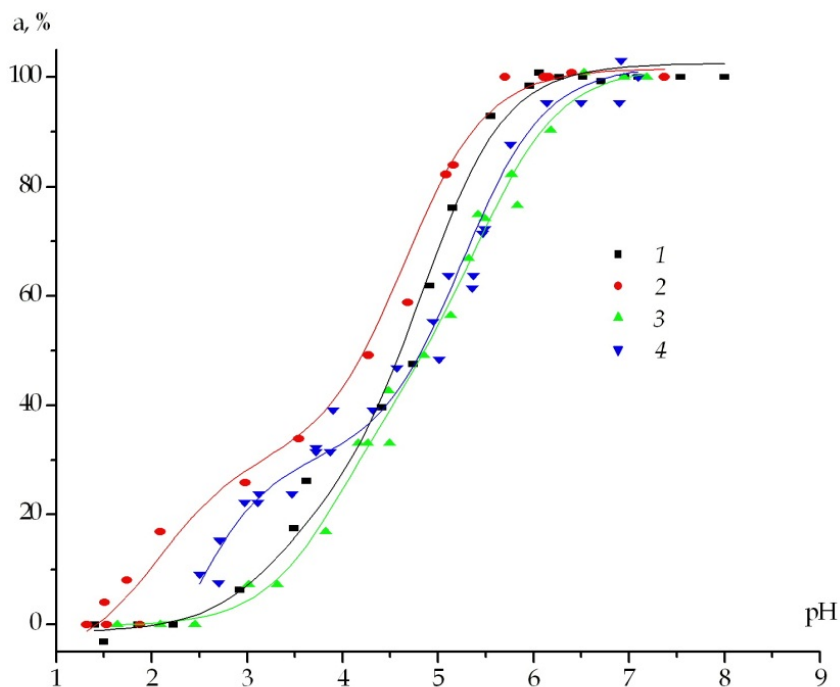


Figure 15. Titration curve for NR R1 in aqueous bulk solution (calibration curve) (1), near the surface of MCC (2), of the hybride MCC- chitosan (3), of the MCC- chitosan- Co^{2+} (4) systems . $a, \% = ((a-\text{aNRH}^+)/(\text{aNR}-\text{aNRH}^+)) \times 100\%$

This is in complete agreement with the relative positions of the radical titration curves for Al_2O_3 and Al_2O_3 -chitosan. It must be emphasized that the pK_a dissociation value of hydroxyl groups of Al_2O_3 is higher, and lies outside the radical sensitivity range.

Deposits of chitosan on the MCC substrate breaks it into smaller particles (Table 2), due most likely to the recharging of the surface from positive to negative. Chitosan molecules are appreciably smaller in size than MCC molecules, that is why a negative charge leads to increased repulsion inside large MCC particles, to their disintegration, and finally to an increase in the total surface area of the material. Chitosan thus plays the role of a disaggregating surfactant. In case of inorganic substrates, the deposition of chitosan leads to an increase in the particle size, and consequently to a decrease in their surface area (Table 1). Chitosan is therefore a weakly aggregating surfactant as to inorganic substrates.

The pK_a value for amino groups of chitosan is 6.42 (Skorik et.al, 2003). In the investigated pH range ($\text{pH} \leq 6$), polymer molecules must consequently be positively charged due to the formation of $-\text{NH}_3^+$ ammonium groups. If chitosan molecules were adsorbed on the surface of inorganic oxides so that the protonated amino groups were on the material surface, this kind of adsorption would be reflected in the titration curves of the modified samples and

would cause the titration curve to shift to the left of the titration curves of the initial oxides. Since this did not happen, we can assume that during the formation of hybrid material, chitosan amino groups form weak hydrogen bonds or Van der Waals bonds with functional groups of substrates (organic or inorganic), leading to an arrangement of chitosan molecules in which glucosamine rings are turned in the direction of the substrate.

3.4.2. Co^{2+} -containing hybrid systems

The presence on the support surface of a polymer that is capable of acquiring metal ions of high coordination numbers is needed to fix these ions more firmly on metal-containing hybrid materials. This role was played by chitosan on the surfaces of the inorganic (SiO_2 , Al_2O_3) and organic (MCC) supports. Co^{2+} ions were sorbed from an aqueous ethanol solution (Fig. 16).

The composition of the studied systems was characterized by elemental analysis. According to the data, the sorption capacity of the hybrid systems relative to Co^{2+} ions is different and declines in the following order: $\text{SiO}_2 > \text{Al}_2\text{O}_3 > \text{MCC}$. We should note that in this case, there is a difference between the mechanisms of binding ions for different supports, since their surfaces have the same coating influencing the process.

As follows from the elemental analysis, chitosan plays the role of a complexing agent. In this case, all amino groups are involved in the coordination by cobalt ions (ratio $\text{Co}:\text{NH}_2 = 1:1-1.5$).

In the case of the Al_2O_3 -chitosan system, some of the amino groups do not participate in the complexation, but the $\text{Co}:\text{Cl}$ ratio corresponds to the composition of the initial salt that provides the coordination mechanism for binding cobalt ions (Fig.17). In the case of the SiO_2 -chitosan system, the $\text{Co}:\text{Cl}$ ratio is ~ 1 . The need to obey the law of electroneutrality for the obtained hybrid systems requires assuming that the support, in addition to being a weak acid, also plays a coordinating role with respect to Co^{2+} ions, which accords with the covalent mechanism of binding Co^{2+} ions (Fig. 17). In the case of the MCC-chitosan system, metal ions are sorbed as a basic salt, and hydroxyl groups on the surface provide weaker coordination binding than Al_2O_3 .

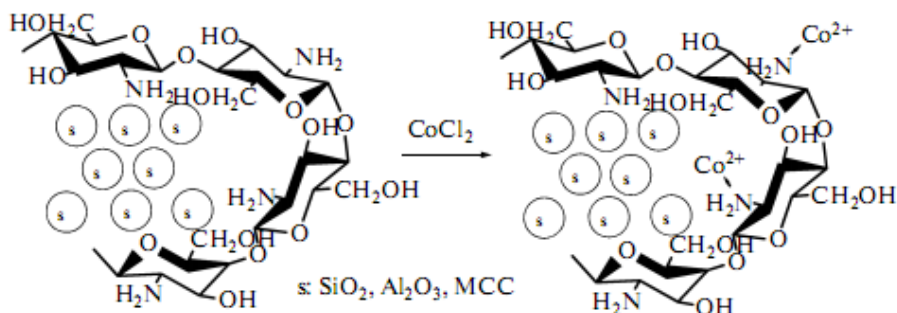


Figure 16. Scheme for synthesis of cobalt-containing hybrid systems. s - support

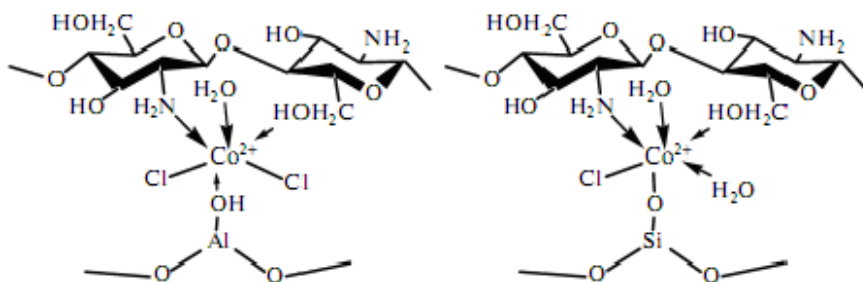


Figure 17. Scheme for the mechanism of binding Co^{2+} by hybrid systems

The elemental composition of the surface shows that chitosan does not cover it completely and some part of the functional groups remains on the support surface in free form. The more complex structure of the surface of hybrid system was characterized by investigating its acid–base properties via ESR spectroscopy of the NR used as pH probes. The titration curves of NR R1 on the surface of the Co^{2+} -containing system are shown in Figs. 13–15. The shift in these curves relative to the calibration curve left or right allows us to determine whether the surface has a positive or negative charge, respectively (Kovaleva et al., 2000 ; Molochnikov et al., 2007).

The technique for introducing Co^{2+} ions into the hybrid materials from the ethanol solutions could lead to the formation of sediments of basic cobalt chloride or chloride–alcoxide micelles on the surface of these materials. In the case of the MCC–chitosan (Fig. 15) and Al_2O_3 –chitosan (Fig. 13) systems, the titration curves of the cobalt-containing materials at $\text{pH} > 5$ are shifted slightly to the left relative to the titration curves of the initial samples. Consequently, the occurrence of basic cobalt chloride on the surface of these materials does not lead to a change in the surface charge, but changes its value slightly. This is due to the effective neutralization of a positive charge of Co^{2+} ions by negative chloride and hydroxide ions. In order to confirm our hypothesis, we present the published data on studying the sorption of Co^{2+} ions from aqueous solutions and on the nature of the interaction between the metal center and amino groups of chitosan. According to (Minimisawa et al., 1999) maximum adsorption starts to decrease with increasing pH due to the formation of cobalt hydroxocomplexes. The maximum sorption of cobalt ions by chitosan found at pH 6–8 in (Silva et al., 2008) is in good agreement with the data from (Minimisawa et al., 1999) and is determined by the formation of $\text{Co}(\text{OH})_2$ phase or slightly soluble basic salts. No chemical interaction with amino groups of chitosan occurs in this case (Zhao et al., 1998).

The SiO_2 –chitosan system behaves differently. Even at the highest pH values, the titration curve of the sample modified with cobalt (Fig. 17) was appreciably shifted to the left relative to the NR curve of the initial sample, although it remains to the right of the calibration curve. Accordingly, the formation of the chloride hydroxyl cobalt micelles immediately leads to a considerable reduction in the negative surface charge of the SiO_2 –chitosan system. The different behavior of the titration curve for system III (Table 2) is most likely associated

with the initially lower amount of Cl^- ions in the cobalt micelles ($\text{Co} : \text{Cl} = 1 : 1$), i.e., to its higher amount of OH^- ions. Acid sites on the SiO_2 surface (silanol groups) also likely interact with the basic cobalt chloride particles precipitating on the surface, thereby replacing the Cl^- ions. In both cases, the titration curve must shift left due to the neutralization of the negative surface charge. In the study of the samples in the aqueous medium at high pH values, the transformation for systems I–III (Table 2) thus occurs; hydration of the surface, followed by hydrolysis leading to the formation of colloidal particles based on chloro-hydroxo complexes of Co^{2+} ions, is observed.

These micelles of Co^{2+} chloro-hydroxocomplexes begin to dissolve at $\text{pH} \leq 5$ for all investigated systems. The dependence of sorption of cobalt ions on pH (Minimisawa et al., 1999) shows that the maximum adsorption starts to decline at $\text{pH} < 5$, and Co^{2+} ions in the solution are in the form of aqua complexes (Zhao et al., 1998). The latter are sorbed by the chitosan primary amino groups, thereby charging the surface positively; in this case, the titration curves of systems I–III (Table 2) (Figs.13-15) are shifted left relative to the corresponding curves for the initial samples and to the calibration curve. A further reduction in pH leads to the neutralization of OH^- groups, and no further changes in pH near the particle surface are observed upon a change in pH_{ext} .

This indicates the presence of a horizontal plateau on the titration curve. The value of the horizontal section is lower for system III than for systems I and II (Table 2), since some of the OH^- groups are replaced by residues of silicic acid. At high pH values, Co^{2+} ions initially cause a substantial decrease in the negative surface charge for the case of system III; their transformation into the form coordinated by the chitosan - NH_2 groups thus influences the surface charge to a lesser degree upon declining pH. Our results indicate the participation of chitosan amino groups in the complexation with Co^{2+} ions. During the interaction of the hybrid materials with the Co^{2+} -containing solution, at least a part of glucosamine rings are consequently turned outward and are capable of becoming ligands.

4. Conclusions

pH-sensitive NRs gave reliable information on the local acidity of solutions in and the charge of a surface on pure and metal containing inorganic and organo-inorganic materials and systems and allowed to estimate an electric potential near the surface of TiO_2 nanoparticles.

The differences between the acidities of external solutions (pH_{ext}) and inside pores (or near the surface) of all the studied materials and systems (pH_{int}) were found.

The method of spin pH probes allowed to determine the ionization constants of characteristic functional groups of SiO_2 -based systems from the horizontal plateaus corresponding to the constant pH_{int} in the samples.

An increase in concentration of H^+ ions (a decrease in pH_{int}) in solutions located inside $\alpha\text{-Al}_2\text{O}_3$, TiO_2 hydrogel and near the surface of the BS-50 type SiO_2 , TiO_2 and SiO_2 xerogels ; the

related CMs and hybrid materials; metal-containing systems, as compared to those of external solution can be explained by releasing H^+ ions due to dissociation of acidic functional groups, exchange them with metal ions and the partial disruption of hydrogen bonds. It leads to negative charge of a surface of the above-mentioned objects. A decrease in concentration of H^+ ions (an increase in pH_{int}) as compared to those of external solution were characteristic for $\gamma-Al_2O_3$ and cellulose matrixes. This resulted from binding H^+ -ions by the surface of $\gamma-Al_2O_3$ and MCC and PC with basic functional groups such as $-AlOH$, $-AlO^-$ and OH^- , respectively. As a result, a surface gains a positive charge.

The sorption capacity of Cu^{2+} ions depends on a surface charge of the oxides gels, xerogels and the related CMs studied and decreases as a negative surface charge reduces. The sorption of Cu^{2+} ions on the surface of nanoparticles of nanostructural TiO_2 increases the charge of the latter. An increase in a percentage of PC in the SiO_2 -PC composites leads to an increase in the amount of silanol groups as a result of increasing in dispersivity of SiO_2 particles and specific surface (S_{sp}) of the samples, and to reducing a negative surface charge up to zero, and even its reversing. It led to the formation of $Cu(OH)_2$.

The deposition of chitosan on the substrate always creates a negative charge on the surface. While the deposition of chitosan leads to relatively slight changes in the surface potential in the case of inorganic substrates such as Al_2O_3 and SiO_2 , these changes are so great in the case of MCC that they even lead to changes in the surface charge.

The charge of the surface of Co^{2+} -modified organo-inorganic hybrid materials at different pH_{int} was found to effect on the composition and structure of Co^{2+} -containing surface compounds.

The modification of a surface of powder cellulose with nanostructured SiO_2 and TiO_2 xerogels, aluminum oxides, silica and MCC with acidic functional groups and chitosan makes it possible to adjust the local acidity and surface charge over a wide range.

The study of the surface of organo-inorganic composites and hybrid materials and systems using pH-sensitive nitroxyl radicals allows also to reveal regularities in changing their properties during further modification. In addition, this method enables us to describe qualitatively the processes of structure formation in these systems and their effect on catalytic activity in different pH-dependent reactions.

The calculated φ value (31.7 mV) was found not to be the electric potential of TiO_2 nanoparticle surface, but it only characterizes the electric field generated by a nanoparticle at the site where the radical fragment $-N-O\bullet$ of NR is located. Once the anisotropic spectra of NR in nanostructured oxides are simulated, an electrical potential of a surface can be determined. When measuring the SEP of solids, the knowledge of the distance between a radical and a surface is of principal importance. The fixation of pH-sensitive NRs on the surface of nanoparticles with linkers of a known length can solve this problem. This will allow one to calculate the potential immediately on the surface of nanoparticles and to compare the calculation results with the experimental data on the electrokinetic potentials.

Author details

Elena Kovaleva*

Ural Federal University, Russia

Leonid Molochnikov

Ural State Forest Engineering University, Russia

Acknowledgement

The authors are very grateful to :

- Prof. A.M. Volodin and Prof. A.I. Kulak for synthesizing and supplying aluminum oxides and nanostructured TiO₂ both original and modified with F⁻ and SO₄²⁻ groups,
- Dr. I.A. Kirilyuk and Prof. I.A. Grigor'ev for synthesis of pH-sensitive nitroxide radicals,
- Dr. A.B. Shishmakov, Mrs. Yu. V. Mikushina and Dr. E. V. Parshina for synthesizing TiO₂ and SiO₂ hydrogels and xerogels, pure and Cu²⁺-containing solid-phase composites based on nanostructured SiO₂ and TiO₂ and powder cellulose,
- Mr. A.V. Mechaev for synthesis and characterization of pure and Co²⁺-containing hybrid organo-inorganic materials based on the chitosan-SiO₂, chitosan- Al₂O₃, and -chitosan-cellulose systems,
- Prof. A.I. Kokorin , Dr. A.V. Pestov and Prof. Yu.G. Yatluk for fruitful discussion of the study results.

The studies presented in this manuscript were financially supported by the Ministry of the Education of the Russian Federation (2007-2011, Theme 01.2.007-06425).

5. References

- Airoldi C. & Monteiro, O. A. C. (2000). Chitosan-Organosilane Hybrides-Synthesis, Characterization, Copper Adsorption and Enzyme Immobilization. *J. Appl. Polym. Sci.*, Vol. 77, No.4, (July 2000), pp. 797 -804, ISSN 1097-4628
- Borbat, P.P., Milov, A.D., Samoilova, R.I. et al. (1990). Vliyanie Razmera Por na Vrashchatel'nuyu Podvizhnost' Spinovogo Zonda v Silikagel'ach (Effect of Pore Size on Rotational Motion of Spin Probe in Silica Gels). *Kolloidn. Zh. (Russ. Colloid J.)*, Vol. 52, No.2, (February 1990), pp. 341-345, ISSN 1061-933X (in Russian)
- Budanova, N. Yu., Shapovalova, E. N. & Lopatin, S. A. (2001). Issledovanie Uderzhivayushchei i Razdelyayuschei Sposobnosti Silikagelei, Modifitsirovannykh Novym Chiral'nym Selektorom – Nizkomolekulyarnym Khitosanom (Study of Retentivity and Separating Capacity of Silica Gels Modified With a Novel Chiral

* Corresponding Author

- Selector – Low Molecular Chitosan) *Vestn. Mosk. Univ., Ser. Khim.* Vol. 42, No.2, pp.112-115, ISSN 0579-9384 (in Russian)
- Buyanov, R.A.(Ed.).(1998). *Kataliz i Katalizatory: Fundamental'nye Issledovaniya Instituta kataliza im. G.K. Boreskova Sib. Otd. Ross. Akad. Nauk (Catalysis and Catalysts. Fundamental Works of Boreskov Institute of Catalysis)*, Siberian Branch of the Russian Academy of Sciences, ISBN 5769201320, Novosibirsk, Russia (in Russian)
- Corma A., Concepción, P., Domínguez, I. et al. (2007). Gold Supported on a Biopolymer (Chitosan) Catalyzes the Regioselective Hydroamination of Alkynes. *J. Catal.*, V.251, No. 1, (1 October, 2007), pp. 39-47, ISSN 0021-9517
- Fromherz, P. (1989). Lipid Coumarin Dye as a Probe of Interfacial Electrical Potential in Biomembranes. *Methods Enzymol.*, Vol. 171, pp. 376-387, ISSN 0076-6879
- Golovkina, E.L., Kovaleva, E.G., Molochnikov, L.S. et al. (2008). Method of Spin Probe for Study of MMS SBA-15. *Zhurnal Khromatographicheskikh I Sorbtsyonnykh Processov (Russ.J. Sorp. Chromat. Proc.)*, Vol. 8, No. 6, (June 2008), pp. 971-985, ISSN 1680-0613 (in Russian)
- Golovkina E. L. (2009). Electrochemical Properties of Mesoporous Molecular Sieves : Measurements and Study Using Spin pH-probe Method, Ph. D. Dissertation in Chemistry, Ural State Forest Engineering University, Yekaterinburg, Russia (defended at the Chelyabinsk State Pedagogical University, Chelyabinsk) (in Russian)
- Griffith, O.H., Dehlinger, P. J. & Van, S. P. (1974). Shape of the Hydrophobic Barrier of Phospholipid Bilayers (Evidence for Water Penetration in Biological Membranes). *J. Membrane Biol.* V.15, No.1, (December 1974), pp. 159-192, ISSN 0022-2631
- Hubbard, E.T., (Ed.) (2002). *Encyclopedia of Surface and Colloid Science*, Marcel Dekker, ISBN, New York
- Huang, K., Liu, H., Dou, X. et al. (2003). Silica-Supported Chitosan-Osmium Tetroxide Complex Catalysed Vicinal Hydroxylation of Olefins Using Hexacyanoferrate (III) Ion as a Cooxidant. *Polym. Adv. Technol.*, Vol. 14, No.4, (April 2003), pp. 366-370, ISSN 1099-1581
- Iller, R. (1979). *The Chemistry of Silica*, Wiley, New York
- Jeon, J.S., Sperline, R.P., Raghavan, S. et al. (1996). In Situ Analysis of Alkyl Phosphate Surfactant Adsorption at the Alumina/Aqueous Solution Interface. *Colloids Surf., A*, Vol. 111, No.1, (June 1996) , pp. 29, ISSN 0927-7757
- Khan, R., Kaushik A., Solanki, P. R. et al. (2008). Zinc Oxide Nanoparticles-Chitosan Composite Film for Cholesterol Biosensor. *Anal. Chim. Acta* , Vol. 616, No.2, (June 2008), pp. 207-213, ISSN 0003-2670
- Kharchuk, V.G., Buldakova, L.Yu., Shishmakov, A.B., et al. (2004). Oxidative Dehydrogenation of 2,3,5-Trimethyl-1,4-Hydroquinone in the Presence of Titanium Dioxide Hydrogel. *Russ.J. General Chem.*, Vol. 74, No.1, (January 2004), pp. 101-104, ISSN 1070-3632
- Khramtsov V. & Weiner L. (1988). Proton Transfer Reactions in Free Radicals. Spin pH probes. *Uspekhi Khimii (Russian Chem. Rev.)*, Vol. 57, No.9, (September 1988), pp. 824-832, ISSN 0036-021X (in Russian)

- Khramtsov, V.V., Marsh, D., Weiner, L.M., et al. (1992). The Application of pH-sensitive Spin Labels to Studies of Surface Potential and Polarity of Phospholipid Membranes and Proteins. *Biochim. Biophys. Acta*, Vol. 1104, pp. 317-324, ISSN 0006-3002
- Khramtsov, V.V. & Volodarsky, L.B. (1998). Use of Imidazoline Nitroxides in Studies of Chemical Reactions: ESR Measurements of the Concentration and Reactivity of Protons, Thiols and Nitric Oxide. In : *Biological Magnetic Resonance, Vol. 14, Spin Labeling*, Berliner, L., Ed., p. 109-180, Plenum Press, ISBN 0306456443, New York
- Kirilyuk, I.A., Bobko, A. A. Khramtsov, V. V. & Grigor'ev, I. A. (2005). Nitroxides with Two pK Values-useful Spin Probes for pH Monitoring Within a Broad Range. *Org. Biomol. Chem.* Vol.3, No. 7, pp. 1269-1274, ISSN 1477-0520
- Kovaleva, E.G., Molochnikov, L.S. & Lipunov, I.N. (2000). The Influence of the Mixed H⁺-Na⁺ Form of KB- 2 Carboxyl Cationite and of pH within Ionite Grains on the State of Cu(II) Ions and the Catalytic Properties of Ionite Catalysts Containing Cu(II). *Rus.J.Phys. Chem.*, Vol. 74, No.8, (August, 2000), pp. 1262-1267, ISSN 0036-0244
- Lidin, R.A., Andreeva, L.L. & Molochko, R.A. (1987). *Spravochnik Po Neorganicheskoi Khimii (Handbook on Inorganic Chemistry)*, Khimiya (Chemistry) ISBN 5-7245-1163-0, Moscow (in Russian)
- Lisichkin, G.V., Fadeev, A.Yu., Serdan, A.A. et al. (2003) *Khimiya Pryvitykh Poverkhnostnykh Soedinenii (Chemistry of Graft Surface Compounds)*, FIZMATLIT , ISBN 978-5-9221-0342-8, Moscow, Russia (in Russian)
- Li, G., Jiang, Y., Huang, K., Ding, P. et al. (2008). Preparation and Properties of Magnetic Fe₃O₄-chitosan Nanoparticles. *J. Alloys Compd.*, Vol. 466, No.2, (October 2008), pp. 451-456, ISSN 0925-8388
- Liu, X. Tokura D. S. & Haruki, M. (2002). Surface Modification of Nonporous Glass Beads with Chitosan and Their Adsorption Property for Transition Metal Ions. *Carbohydr. Polym.*, Vol. 49, No.1, (July 20012), pp. 103-108, ISSN 0144-8617
- Long, Y., Xu, T., Sun, Y. et al. (1999). Adsorption Behavior on Defect Structure of Mesoporous Molecular Sieves. *Langmuir*, Vol.15, No.19, (September 1999), pp. 6173-6178, ISSN 0743-7463
- Martini, G., Bindi, M., Ottaviani, M.F., et al. (1985). Dipolar and Spin Exchange Effects in the ESR Spectra of Nitroxide Radicals in Solution: Part II. Water Solutions Adsorbed on Porous Silica Gels. *J.Colloid Interface Sci.* , Vol. 108, No.1, (November 1985), pp. 140- 148, ISSN 0021-9797
- Mei, N., Xuguang, L., Jinming, D. et al. (2009). Antibacterial Activity of Chitosan Coated Ag-loaded Nano-SiO₂ Composites. *Carbohydr. Polym.*, Vol. 78, No.1, (August 2009), pp. 54-59, ISSN 0144-8617
- Mekhaev, A.V., Pestov, A.V., Molochnikov, L.S. et al. (2011). Investigation of the Structure of Chitosan Hybrid Systems by pH-sensitive Nitroxide Radical. *Russ. J. of Phys. Chem. A*, Vol. 85, No.6, (June 2011), pp. 987-992, ISSN 0036-0244
- Mekhaev, A.V, Pestov, A.V., Molochnikov, L.S. et al. (2011). Structure and Characteristics of Chitosan Cobalt-Containing Hybrid Systems, the Catalysts of Olefine Oxidation. *Russ. J. Phys. Chem. A*, Vol. 85, No.7, (July 2011), pp. 1155-1161., ISSN 0036-0244

- Méndez, A.L, Bosch, Roses M. & Neue, U. D. (2003). Comparison of the Acidity of Residual Silanol Groups in Several Liquid Chromatography Columns. *J. Chromatogr. A*, Vol.986, No.1, (January 2003), pp. 33–44, ISSN 0021-9673
- Mininisawa, H., Iwanami, H., Azai, N. et al. (1999). Adsorption Behavior of Cobalt(II) on Chitosan and Its Determination by Tungsten Metal Furnace Atomic Absorption Spectrometry. *Anal. Chim. Acta.*, Vol. 378, No.3, (January 1999), pp. 279-285, ISSN 0003-2670
- Molochnikov, L.S., Kovalyova, E.G., Grigor'ev, I.A. et al. (1996). Determination of Acidity in the Interior of the Cross-linked Polyelectrolyte Grain by the Use of pH-Sensitive probes, In *Metal-Containing Polymeric Materials*, Pittman, Ch.U. et al., pp. 395-401, Plenum Press, ISBN 10 0306452956, New York
- Molochnikov, L. S., Kovalyova, E.G., Golovkina E.L. et al. (2007). Method of Spin Probe for Studying Acidity of Inorganic Materials. *Russ.Colloid J. B*, Vol. 69, No.6, (December 2007), pp. 769-776, ISSN 1061-933X
- Molochnikov, L.S., Kovalyova, E.G., Grigor'ev, I.A., et al. (2004). A Direct Measuring of H⁺ Activity Inside Cross-Linked Functional Polymers. *J. Phys. Chem. B*, 2004, Vol. 108, No.4, (December 2004), pp. 1302-1313, ISSN 1520-6106
- Nawrocki, J. (1997). The Silanol Group and its Role in Liquid Chromatography *J. Chromatogr. A*, V. 779, No.1, (August 1997), pp. 29-71, ISSN 1520-6106
- Neue, U. D. (2000). Silca Gel and Its Derivatization, In : *Encyclopedia of Analytical Chemistry*, Meyers, R. A. Ed.. Wiley, ISBN 9780470027318, Chichester.
- Nikitin, N. I. (1962). *Chemistry of Wood and Cellulose*, No ISBN, Nauka, Leningrad, Russia, (in Russian)
- Paradossi, G., Chiessi, E., Cavalieri, F. et al. (1998). Networks Based on Chitosan and Oxidized Cyclodextrin-II. Structure and Catalytic Features of a Copper (II)-loaded Network. *Polym. Gels & Networks*, Vol. 5, No.6, (April 1998), pp. 525-54, ISSN 0966-7822
- Parshina, E.V., Molochnikov, L.S., Kovaleva, E.G. et al. (2011). Medium Acidity and Catalytic Properties of Composite Materials Based on Silica and Titanium and Powder Cellulose in the Presence of Cu²⁺ Ions. *Russ. J. Phys. Chem. A*, Vol. 85, No.3, (March 2011), pp. 452-456, ISSN 0036-0244
- Parshina, E.V. (2011) *Acid-base, Complexation and Catalytic Properties of Solid Phase Composites Based on Dioxide Elements Xerogels and Powder Cellulose*, Ph. D. Dissertation in Chemistry, Ural State Forest Engineering University, Yekaterinburg, Russia (defended at the Chelyabinsk State Pedagogical University, Chelyabinsk) (in Russian)
- Petrov, L.A., Kharchuk, V.G., Shishmakov, A.B. et al. (1998). Oxidation of 2,3,6-Trimethyl-1,4-Benzenediol by Oxygen in the Presence of Oxide Gels. *Russ. J. Org. Chem.*, Vol. 34, No. 7, (July 1998), pp. 344-346, ISSN 1070-4280
- Poznyak, S.K., Pergushov, V.I., Kokorin, A.I., et al. (1999). Structure and Electrochemical Properties of Species Formed as a Result of Cu(II) ions Absorption onto TiO₂ Nanoparticles. *J. Phys. Chem., B*, 1999, Vol. 103, No.8, (February 1999), pp. 1308 – 1515, ISSN 1520-6106

- Robinson, M., Pask, J.A. & Fuerstenau, D.W. (1964). Surface Charge of Alumina and Magnesia in Aqueous Media. *J. Am.Ceram. Soc.*, Vol. 47, pp. 516-520, No. 10, (October 1964), ISSN 1551-2916
- Senso, A., Oliveros, L. & Minguillon, C. (1999). Chitosan Derivatives as Chiral Selectors Bonded on Allyl Silica Gel : Preparation, Characterization, and Study of the Resulting High-Performance Liquid Chromatography Chiral Stationary Phases. *J. Chromatogr., A*, Vol. 839, No.1, (April 1999), pp.15-21, ISSN 0021-9673
- Silva, R.B., Neto, A.F., Santas, L.S. et al. (2008). Catalysts of Cu(II) and Co(II) Ions Adsorbed in Chitosan Used in Transesterification of Soy Bean and Babassu Oils – A New Route for Biodiesel Syntheses. *Biores. Technol.*, Vol.99, pp.6793-6798, No.15, (October 2008), ISSN 0960-8524
- Shi, Q.-H. , Tian, Y., Dong, X.-Y. et al. (2003). Chitosan-Coated Silica Beads as Immobilized Metal Affinity Support for Protein Adsorption. *Biochem. Eng.J.* Vol.16, No.3, (December 2003), pp. 317- 322, ISSN 1369-703X
- Shishmakov, A.B., Kharchuk, V.G., Kuznetsova, O.V., et al. (2003). Activity of Elements Dioxides in liquid Phase Oxidation of 2,3,5-trimethyl Hydroquinone. *Zh. Fiz. Khim. (Rus. J. Phys. Chem.)*, Vol. 77, pp. 623-628, ISSN 0036-0244 (in Russian)
- Shishmakov, A. B., Mikushina, Yu. V., Valova, M. S. et al. (2007). TiO₂ Xerogel Modified with Powder Cellulose in Oxidation Trimethylhydroquinone. *Russ. J. Appl. Chem.*, Vol.80, No.12, (December 2007), pp. 2107-2111, ISSN 1070-4272
- Shishmakov, A.B., Kovaleva, E.G., Mikushina, Yu.V. et al. (2010). EPR study of Cu(II)-Complexes in Matrix of the TiO₂ Gel Modified with Powder Cellulose. *Russ. J. Inorg. Chemistry*, Vol. 55, No.6, pp. 937-942, ISSN 0036-0236
- Skorik, Yu. A., Gomes, C. A. R., Teresa, M. , Vasconcelos, S. D. et al. (2003). N-(2-Carboxyethyl) Chitosans : Regioselective Synthesis, Characterization and Protolytic Equilibria. *Carbohydr. Res.* , V.338, No.3, (January 2003), pp. 271-276, ISSN 0008-6215
- Ur'ev, N. B. & Potanin, A. A. (1992). *Tekuchest' suspenzi' i poroshkov (Fluidity of Suspensions and Powders)* Khimiya (Chemistry), ISBN 5724506572, Moscow (in Russian)
- Varghese, J. G., Karuppanan, R. S. & Kariduraganavar, M. Y. (2010). Development of Hybrade Membranes Using Chitosan and Silica Precursors for Pervaporation Separation of Water + Isopropanol Mixtures. *J. Chem. Eng. Data*, Vol. 55, No.6, (June 2010), pp. 2084-2092 , ISSN 0021-9568
- Varma, A. J. , Deshpande, S. V.& Kennedy, J. F. (2004). Metal Complexation by Chitosan and Its Derivatives : A Review. *Carbohydr. Polym.* Vol. 55, No.1, (January 2004), pp. 77-93, ISSN 0144-8617
- Viswanathana, N. & Meenakshib, S (2010). Enriched Fluoride Sorption Using Alumina-Chitosan Composite. *J. Hazard. Mater.* Vol. 178, No.1, (June 2010), pp. 226-232, ISSN 0304-3894
- Voinov, Maxim A., Kirilyuk, Igor A. & Smirnov, Alex I. (2009). Spin-Labeled pH-Sensitive Phospholipids for Interfacial pK Determination: Synthesis and Characterization in Aqueous and Micellar Solutions. *J. Phys. Chem. B*, Vol.113, No. 11, (March 19, 2009), pp.3453–3460, ISSN ISSN 1520-6106

- Volodarskii, L.B., Grigor'ev, I.A., Dikanov, S.A. et al. (1988). *Imidazolinovye Nitroksil'nye Radikaly (Imidazoline Nitroxyl Radicals)*, Nauka, ISBN 5-0028677-X, Novosibirsk (in Russian)
- Xue, L., Zhou, D.-J., Tang, L. et al. (2004). The Asymmetric Hydration of 1-octene to (S)-(+)-With a Biopolymer-Metal Complex, Silica-Supported Chitosan-Cobalt Complex. *React. Funct. Polym.* Vol.58, No. 2, (February 2004), pp. 117 - 121 , ISSN 1381-5148
- Yeh, J. Chen, C. & Huang, K. (2007). Synthesis and Properties of Chitosan/SiO₂ Hybride Materials. *Mater. Lett.* ,Vol. 61, No.6 , (March 2007), pp.1292- 1295.,ISSN 0167-577X
- Zakharova, G.S., Volkov, V.L., Ivanovskaya, V.V. et.a l. (2005). *Nanotrubki i Rodstvennyye Nanostrukturny Oksidov Metallov (Nanotubes and Related Nano-structures of Metal Oxides)*, Ural. Otd. Ross. Akad. Nauk (Ural Branch of the Russian Academy of Sciences), ISBN 5-7691-1559-9, Yekaterinburg (in Russian)
- Zamaraev, K.I., Salganik, R.I., Romannikov, V.N. et al. (1995). Modeling of Prebiotic Oligopeptides in the Presence of Zeolites and Kaolin as Catalysts. *Dokl. Akad. Nauk* (Reports of Academy of Sciences), Vol. 340, p. 779-782, ISSN 0869-5652 (in Russian)
- Zhang, J. & Xia, C. (2003). Natural Biopolymer-Supported Bimetallic Catalyst Ssystem for the Carbonylation to Esters of Napoxen. *J. Mol. Catal. A: Chem.* Vol.206, No.1, (October 2003), pp. 59-65, ISSN 0021-9517
- Zhao, X. S. & Lu, G. Q. (1998). Modification of MCM-41 by Surface Silylation with Trimethylchlorosilane and Adsorption Study. *J. Phys. Chem. B*, Vol. 102, No.9, (February 1998), pp.1556-1561, ISSN 1520-6106
- Zhao, X. S., Lu, G. Q., Whittaker, A. K. et al. (1997). Comprehensive Study of Surface Chemistry of MCM-41 Using ²⁹Si CP/MAS NMR, FTIR, Pyridine-TPD and TGA. *J. Phys. Chem. B*, V. 101, No.33, pp. 6525-6531, ISSN 1520-6106